Time as a Projection Rate: A 4D Quantum Framework for Temporal Emergence

Mazen Zaino
ORCID: 0009-0002-3862-6407

Oct 16, 2025, Dubai, UAE

Abstract

We propose a novel interpretation of time as an emergent phenomenon arising from the rate at which a four-dimensional (4D) quantum structure projects into three-dimensional (3D) classical space. Unlike conventional approaches in general relativity and quantum mechanics, which treat time as either a fundamental coordinate or an external parameter, our framework derives temporal flow from the decoherence-driven projection of a higher-dimensional quantum configuration onto a 3D observational frame [1, 2].

This projection occurs in discrete increments, defined as *Projection Frame Units* (PFUs), which constitute the fundamental building blocks of temporal measurement. In typical decohered laboratory systems, the duration of a PFU is estimated to be on the order of 10^{-21} s, many orders of magnitude above the Planck time but still below directly accessible experimental resolutions. Classical time intervals emerge from the accumulation of PFUs along entropy gradients, establishing a quantitative link between temporal flow and thermodynamic irreversibility [3].

The framework suggests two experimentally accessible consequences. First, it predicts measurable deviations in quantum tunneling delay times, where PFU modulation alters sub-attosecond transit dynamics. Second, it implies the possibility of high-frequency gravitational-wave transients produced by rapid deprojection events near black hole horizons. Both signatures are in principle testable with current or near-future experimental platforms, including attosecond interferometry and next-generation gravitational-wave detectors [5, 6].

By rooting time in the informational and geometric structure of quantum projections, this approach provides a falsifiable path toward unifying quantum mechanics, gravitational dynamics, and the thermodynamic arrow of time within a higher-dimensional paradigm.

Contents

https://doi.org/10.33774/coe-2025-brblf-v2 **ORCID:** https://orcid.org/0009-0002-3862-6407 Content not peer-reviewed by Cambridge University Press. **License:** CC BY 4.0

1 Introduction

The nature of time remains one of the most profound and unresolved problems in theoretical physics. Across classical, relativistic, and quantum frameworks, time plays fundamentally distinct roles, and attempts to reconcile these divergent treatments have exposed deep conceptual tensions. In Newtonian mechanics, time is absolute, universal, and flows independently of the system under consideration. This view was revolutionized by Einstein's theory of relativity, which replaced absolute time with a flexible, coordinate-dependent quantity embedded in the four-dimensional spacetime continuum [7].

In general relativity, the temporal coordinate is local and malleable, shaped by spacetime curvature induced by mass-energy distributions. However, when transitioning to quantum gravity, particularly in canonical quantization and quantum cosmology, time loses even this local status. In the Wheeler–DeWitt equation, for instance, there is no explicit time variable, giving rise to the "problem of time" in quantum gravity [8, 9]. This absence challenges our understanding of change, causality, and evolution in quantum systems.

Within standard quantum mechanics, time remains a classical parameter driving unitary evolution via the Schrödinger equation. This asymmetry, where space is quantized but time is not, disrupts spacetime uniformity and highlights a conceptual gap in the completeness of existing theories. Furthermore, the directional flow of time, manifested in the thermodynamic arrow and entropy increase, is not naturally incorporated in either quantum theory or general relativity, both of which are fundamentally time-reversal invariant [3, 10].

A number of emergent-time proposals attempt to resolve these issues. The Page–Wootters mechanism defines time relationally, as an entanglement parameter within a larger stationary state. The Thermal Time Hypothesis identifies time flow with the modular Hamiltonian of a system's statistical state [3]. Causal Set Theory, in contrast, derives temporal order from the discrete structure of spacetime itself. While conceptually powerful, these approaches remain limited in testability: they provide frameworks for interpretation, but few concrete, falsifiable predictions.

In this work we propose an alternative route. Time is identified with the rate at which a four-dimensional (4D) quantum geometry undergoes decoherence-driven projection into a three-dimensional (3D) observational frame. This process is intrinsically linked to entropy flow and coherence loss, making the emergence of time both observer-dependent and thermodynamically aligned. Projection Frame Units (PFUs) serve as the fundamental increments of this process. PFUs differ from earlier proposals because they connect decoherence and entropy gradients directly to temporal increments, thereby producing experimentally accessible predictions, for example, measurable deviations in tunneling delay times and transient gravitational-wave bursts.

A potential circularity arises because PFUs appear to be defined with respect to classical time intervals. We resolve this by grounding PFUs in decoherence dynamics: the unit is defined by discrete increments of entropy-driven projection, independent of classical t. Standard temporal coordinates only appear when mapping PFUs to conventional units such as seconds. In this way, classical time is recovered as an emergent bookkeeping device rather than an input.

To formalize this framework, we develop a tensor-based mathematical structure incorporating projection operators, generalized Schrödinger evolution, and entropy-gradient equations. This allows PFUs to be embedded consistently into both quantum dynamics and relativistic spacetimes.

The main contributions of this work are as follows:

- We provide a coherent conceptual framework linking the emergence of time to 4D quantum projection and thermodynamic irreversibility.
- We formalize the notion of PFUs as discrete temporal units connected to quantum decoherence and entropy gradients.
- We derive falsifiable predictions, focusing on tunneling delay anomalies and high-frequency gravitational-wave transients.
- We situate our framework relative to existing emergent-time approaches, highlighting both conceptual distinctions and testable consequences.

The paper is organized as follows. Section 2 develops the conceptual foundation of time as a projection process and introduces PFUs. Section 3 presents the mathematical formalism, including projection tensors, decoherence rates, and entropy-driven temporal dynamics. Section 4 explores physical implications, including black hole horizons, photon trajectories, and relativistic time effects. Section 5 details testable predictions and potential experimental approaches. Section 6 contrasts our framework with contemporary theories of quantum gravity and emergent time. Finally, Section 8 summarizes key insights and outlines directions for future research.

By framing time as an emergent, quantized feature of a higher-dimensional quantum reality, this work provides a unified lens for understanding its geometric, thermodynamic, and quantum aspects.

Notation and units (definitions used throughout):

1. $N(x)$: integer count of PFUs experienced by a worldline or system; dimensionless.

2. δ : characteristic PFU duration in seconds; units: s.

3. $\Gamma(x)$: PFU production rate, $\Gamma \equiv dN/dt$; units: s^{-1}.

4. τ : emergent proper time measured in seconds. Relationship used in this paper: $d\tau = \delta\, dN = \delta\, \Gamma\, dt$.

5. t : coordinate time used in metric expressions; units: s.

2 Conceptual Foundations

In this section, we establish the theoretical framework for interpreting time as an emergent phenomenon arising from the projection of a four-dimensional (4D) quantum structure into three-dimensional (3D) classical reality. Our approach is grounded in the dynamics of quantum coherence, decoherence rates, and entropy flow, and introduces a fundamental temporal unit, the *Projection Frame Unit* (PFU), to quantify the discrete steps of this projection process. This allows us to recast classical time intervals as cumulative effects of PFU transitions along defined entropy gradients, linking temporal experience to both information flow and thermodynamic irreversibility.

2.1 Time as a Projection Rate

Time, in our framework, is not a preexisting dimension but emerges from the rate at which a coherent 4D quantum system projects into a decohered 3D classical configuration. To formalize this process, we associate the *projection rate* Γ with the frequency of decoherence-induced transitions that map the hidden 4D structure into observable 3D states.

The reduced density matrix ρ_{3D} evolves according to the general Lindblad master equation:

$$\frac{d\rho_{3D}}{dt} = -\frac{i}{\hbar}[H, \rho_{3D}] + \sum_k \left(L_k \rho_{3D} L_k^\dagger - \tfrac{1}{2}\{L_k^\dagger L_k, \rho_{3D}\} \right), \tag{2.1}$$

where H is the effective Hamiltonian of the reduced system and $\{L_k\}$ are Lindblad operators describing the action of the hidden dimension or environment on the system. The non-unitary part of Eq. (2.1) encodes decoherence and entropy production.

We now define a single *Projection Frame Unit* (PFU) as one effective decoherence "event", that is, a discrete increment in which off-diagonal coherence is suppressed beyond a threshold set by the environment's correlation time. The projection rate Γ is then identified with the rate of such decoherence events:

$$\Gamma \;\equiv\; \lim_{\Delta t\to 0} \frac{\Delta \mathrm{PFU}}{\Delta t} \;=\; \mathrm{Tr}\left[\sum_k L_k^\dagger L_k \, \rho_{3\mathrm{D}}\right]. \tag{2.2}$$

Equation (2.2) grounds Γ directly in the dynamical structure of open quantum systems, avoiding circular reference to classical time. Classical t only reappears when mapping PFU counts onto observer-based units (e.g., seconds) for comparison with experiments. In this sense, Γ is the fundamental quantity, while ordinary time is emergent.

Key features of this approach include:

- **Discrete Temporal Structure:** Each PFU corresponds to a Lindblad-type decoherence increment, providing a microscopic underpinning of temporal discreteness.
- **Link to Thermodynamics:** Since decoherence is tied to entropy production, Γ naturally aligns the flow of time with the thermodynamic arrow.
- **Dependence on Physical Conditions:** Local energy density, coherence levels, and entropy flows determine the magnitude of Γ, offering a unified explanation for time dilation, null-PFU freezing along lightlike trajectories, and other relativistic or quantum temporal effects.

2.2 Projection Frame Units (PFU)

To formalize the emergence of time, we define the **Projection Frame Unit (PFU)** as the minimal discrete increment corresponding to a projection from the coherent 4D quantum manifold into the 3D classical domain. PFUs are context-sensitive; unlike Planck time, their effective duration depends on local physical conditions, including quantum coherence, environmental entanglement, and entropy flow.

Mathematically, the PFU rate $\Delta\tau$ relative to classical coordinate time t is expressed as:

$$\frac{d\tau}{dt} = \frac{1}{\Gamma}, \tag{2.3}$$

where Γ is the local decoherence-driven projection rate. This establishes a direct inverse relationship between time progression and the system's coherence stability.

Worked Example: Single Qubit in a Thermal Bath

Consider a single qubit initially in a coherent superposition state $|\psi\rangle = (|0\rangle + |1\rangle)/\sqrt{2}$, weakly coupled to a thermal environment at temperature T. The reduced density matrix of the qubit evolves under a Lindblad master equation, leading to exponential suppression of off-diagonal elements:

$$\rho_{01}(t) = \rho_{01}(0)\, e^{-t/\tau_d}, \tag{2.4}$$

where τ_d is the decoherence time. For a thermal bath dominated by pure dephasing processes, one obtains

$$\tau_d \approx \frac{\hbar^2}{\lambda^2 k_B T}, \tag{2.5}$$

with λ the system-bath coupling strength.

In our framework, one PFU corresponds to this decoherence interval:

$$\text{PFU} = \tau_d. \tag{2.6}$$

If the bath temperature doubles, $T \to 2T$, the decoherence time halves, $\tau_d \to \tau_d/2$, and consequently the PFU shortens by a factor of two. Thus the projection rate Γ increases, and the local temporal flow accelerates relative to the original conditions.

Key Points

- **Operational Meaning:** PFUs serve as the fundamental unit of temporal evolution in our 4D projection framework.
- **Environmental Dependence:** The PFU duration τ_d is explicitly tied to environmental factors such as bath temperature and coupling strength, demonstrating context-sensitivity.
- **PFU Field as a Local Metric:** Variations in Γ across space define a spatially dependent temporal metric.
- **Connection to 4D Quantum Structure:** PFUs emerge directly from the dynamics of the 4D quantum manifold projecting into classical space.

2.3 Decoherence, Entropy, and Temporal Flow

Entropy gradients provide the directional arrow for projection-induced temporal evolution. Regions of strong entropy increase accelerate the decoherence process, thereby shortening local PFUs and effectively increasing the rate of classical time progression. Conversely, near-zero entropy gradients stabilize coherence, prolong PFUs, and slow temporal flow.

To formalize this relation, we begin with the von Neumann entropy of a system with density matrix ρ:

$$S(\rho) = -\mathrm{Tr}\left[\rho \ln \rho\right]. \tag{2.7}$$

For an open quantum system governed by a Lindblad master equation,

$$\frac{d\rho}{dt} = -\frac{i}{\hbar}[H, \rho] + \sum_k \mathcal{L}_k[\rho], \tag{2.8}$$

the entropy production rate satisfies Spohn's inequality:

$$\frac{dS}{dt} \geq \Phi, \tag{2.9}$$

where Φ denotes the entropy flux into the environment. This inequality guarantees non-negativity of entropy production and provides a rigorous statistical-mechanical basis for the thermodynamic arrow of time.

Within our framework, each *Projection Frame Unit (PFU)* corresponds to a decoherence interval, and the projection rate Γ is naturally linked to entropy production. Specifically, we identify

$$\Gamma \propto \frac{dS}{dt}, \tag{2.10}$$

so that rapid entropy growth corresponds to fast decoherence and shortened PFUs. Substituting into Equation (2.3) gives

$$\frac{d\tau}{dt} \propto \left(\frac{dS}{dt}\right)^{-1}. \tag{2.11}$$

This formalism moves beyond the heuristic $\Gamma \propto |\nabla S|$ relation and grounds the connection in open-system thermodynamics: entropy flux into the environment determines the rate of temporal progression.

Key conceptual points include:

- **Entropy as Temporal Driver:** Projection rate Γ emerges directly from entropy production in the Lindblad framework.
- **PFU Modulation:** Variations in decoherence rate modulate PFUs, providing a quantitative bridge between quantum dynamics and temporal flow.
- **Arrow of Time:** Spohn's inequality guarantees irreversibility, anchoring the emergence of time's directionality in fundamental statistical mechanics.

2.4 Light, Null Projections, and Time Freezing

Photons and other fundamentally massless carriers constitute a limiting case in the projection framework. From the perspective of a classical observer, light follows null geodesics ($ds^2 = 0$) and therefore classically experiences no proper time. In our projection picture this behavior is captured as an effective vanishing of PFU accumulation along the photon's worldline: the effective PFU increment associated with a perfect, non-interacting photon trajectory is taken as zero.

Two clarifications are important. First, the statement that a photon experiences no PFU accumulation is an *idealization*. Physically, any real photon propagating through a medium or an environment will undergo interactions (scattering, absorption, coupling to background fields) that partially decohere its state. Second, the formal vanishing of PFU accumulation should be understood as a limit of the projection-lapse variables used in the main text. Concretely, if $\Lambda(x)$ denotes the local projection lapse that relates emergent proper time to coordinate time (see Section 3), then the null-projection limit is

$$\Delta\mathrm{PFU}\Big|_{\text{ideal photon}} = 0 \qquad \Longleftrightarrow \qquad \Lambda(x) \to 0 \quad \text{along the null path,} \tag{2.12}$$

so that no emergent proper time is accumulated by the photon along that path.

Physical mechanism and finite decoherence. Realistic decoherence of photonic states is governed by their interaction rate with the environment. To first approximation the rate of interactions (scattering or absorption) is

$$\gamma_{\text{int}} \approx n\,\sigma\,c, \tag{2.13}$$

where n is the number density of scatterers, σ is an appropriate cross section and c is the speed of light. When γ_{int} is nonzero the photon's quantum state is subject to environmental monitoring and partial loss of coherence. In the projection picture such interactions generate nonzero PFU increments along the trajectory; conversely, in the limit of vanishing interaction rate (vacuum, negligible background), the PFU increment tends to zero and the null-projection idealization is recovered.

Connection to decoherence theory. This description is consistent with standard open-system treatments of decoherence, in which the reduced dynamics of a photonic subsystem are obtained by tracing out environmental degrees of freedom and the effective decoherence rate is determined by coupling strengths and bath statistics [1, 11]. The crucial point for the PFU framework is that *PFU accumulation along a worldline is controlled by the same physical parameters that determine environmental decoherence*: interaction rates, bath occupation numbers, and scattering cross sections. Thus null-projection is the idealized limit of vanishing environmental coupling.

Observational consequences and caveats. Because real photons in astrophysical or laboratory contexts are never perfectly isolated, one generically expects extremely small but finite PFU contributions along most photon paths. These tiny effects can, in principle, produce subtle phase shifts or coherence loss over long baselines (for example in precision interferometry or in propagation through the interstellar and intergalactic medium). The PFU framework therefore predicts that null-projection is an excellent approximation for nearly free photons in vacuum, but that measurable deviations could appear when photons traverse regions with nonnegligible scattering or background radiation fields.

To summarize:

- The statement “photons do not experience PFU transitions” should be read as an idealized limiting statement; physically it corresponds to negligible environmental coupling.
- Finite photon decoherence is controlled by interaction rates such as Eq. (2.13), which induce nonzero PFU accumulation and therefore small, in-principle observable deviations from perfect null-projection.
- This interpretation aligns with open-system decoherence theory and preserves the main intuition that null geodesics correspond to the limiting case of vanishing emergent proper time.

2.5 PFU–Second Mapping and Classical Time Emergence

To reconcile PFU dynamics with classical temporal measurements, PFU increments are mapped to standard seconds. The mapping under typical terrestrial or laboratory conditions is given by:

$$t_{\text{second}} = N_{\text{PFU}} \cdot \delta, \tag{2.14}$$

where N_{PFU} is the number of PFUs per second and δ is the average PFU duration.

An important step is to estimate δ from known decoherence rates. In mesoscopic or solid-state systems at room temperature, decoherence times typically range from 10^{-20} s to 10^{-18} s depending on environmental coupling strength [11]. Taking a conservative lower bound, we may approximate

$$\delta \sim 10^{-21}\,\text{s}, \tag{2.15}$$

as a characteristic PFU duration in strongly decohered laboratory conditions. This value is many orders of magnitude larger than the Planck time ($t_P \approx 10^{-43}$ s), indicating that PFUs are not fundamental Planck-scale artifacts but rather emergent increments tied to physical decoherence processes.

The precise value of δ depends on context: ultra-coherent superconducting qubits at millikelvin temperatures may yield δ in the range 10^{-15} s or longer, while photons propagating through near-vacuum approximate the null-PFU limit discussed in Section 2.4.

This mapping establishes a bridge between emergent, discrete projection time and classical temporal experience, showing how Newtonian and relativistic time scales arise naturally from the 4D quantum projection framework.

Conceptual highlights:

- **PFU-to-Second Conversion:** Connects the fundamental quantum-projection unit to standard temporal measurement.
- **Order-of-Magnitude Anchor:** In typical laboratory environments, $\delta \sim 10^{-21}$ s, vastly above Planck time but well below everyday time scales.
- **Emergence of Time Scales:** Explains the origin of classical time intervals from PFU progression, supporting both Newtonian and relativistic temporal phenomena.
- **Thermodynamic Alignment:** Ensures consistency with entropy-driven decoherence and the thermodynamic arrow of time.

2.6 Interpretation and Significance

The PFU framework provides a unifying principle for phenomena traditionally treated as distinct. Specifically, PFU modulation underlies both quantum-mechanical and relativistic manifestations of slowed time evolution. In laboratory systems, frequent environmental interactions can suppress PFU advancement, yielding the well-known *quantum Zeno effect* [17]. In gravitational contexts, spacetime curvature alters local decoherence rates, leading to the effective slowing of PFU increments that underpins *gravitational time dilation* [18, 19].

Thus, processes as different as repeated quantum measurement and the influence of gravity on clocks can be interpreted as consequences of a single mechanism: variations in the rate of PFU progression. This perspective consolidates quantum and relativistic time-slowing effects within the same projection-based framework, offering a deeper physical basis for the emergence of time across scales.

3 Mathematical Formalism

This section formalizes the Projection Frame Unit (PFU) framework, treating temporal flow as a derived consequence of quantum-to-classical projection. The central aim is to quantify PFUs through local decoherence dynamics, link them to entropy production, and show how they recover relativistic proper time under limiting conditions. This provides the mathematical infrastructure for embedding projection dynamics into a unified spacetime description.

3.1 PFUs and Quantum Decoherence Dynamics

We begin by defining emergent projection time τ as distinct from the classical coordinate time t. The relation between them is determined by the local decoherence rate $\Gamma(x^\mu)$:

$$\frac{d\tau}{dt} = \frac{1}{\Gamma(x^\mu)}, \tag{3.1}$$

where $x^\mu = (t, \vec{x})$ are spacetime coordinates. Equation (3.1) expresses the principle that temporal flow is not absolute but modulated by the degree of quantum coherence. In regions of suppressed decoherence, $\Gamma \to 0$, projection slows and τ dilates relative to t. In the opposite limit of rapid decoherence, τ advances quickly, recovering the familiar flow of macroscopic time.

Derivation of Γ from Open-System Dynamics. The dynamics of an open quantum system coupled to an environment are governed by the Lindblad master equation [55]:

$$\frac{d\rho}{dt} = -i[H_S, \rho] + \sum_k \left(L_k \rho L_k^\dagger - \tfrac{1}{2}\{L_k^\dagger L_k, \rho\} \right), \tag{3.2}$$

where H_S is the system Hamiltonian, and L_k are Lindblad operators encoding environmental couplings. Tracing over environmental degrees of freedom yields an effective non-unitary evolution, with decoherence rate

$$\Gamma \;\sim\; \sum_k \mathrm{Tr}\Big(L_k^\dagger L_k \rho \Big). \tag{3.3}$$

For weak coupling, $L_k \propto H_{\text{int}}$, so the decoherence rate is proportional to the variance of the interaction Hamiltonian:

$$\Gamma_{\text{dyn}} \;\propto\; \langle \Delta H_{\text{int}}^2 \rangle, \tag{3.4}$$

where $\langle \Delta H_{\text{int}}^2 \rangle = \langle H_{\text{int}}^2 \rangle - \langle H_{\text{int}} \rangle^2$. This captures the *dynamical* contribution: stronger environmental fluctuations drive faster loss of coherence.

Entropy-Gradient Contribution. Beyond dynamical fluctuations, decoherence is also driven by irreversible information flow into the environment. The von Neumann entropy $S = -\mathrm{Tr}(\rho \ln \rho)$ grows monotonically under non-unitary Lindblad evolution. Ex-

https://doi.org/10.33774/coe-2025-brblf-v2 ORCID: https://orcid.org/0009-0002-3862-6407

panding around a local state, the rate of entropy increase can be written

$$\frac{dS}{dt} \sim \nabla_\mu S(x^\mu)\, \dot{x}^\mu, \tag{3.5}$$

so that the magnitude of the entropy gradient, $|\nabla_\mu S|$, quantifies the *thermodynamic* drive toward irreversibility [1, 11]. We therefore identify an entropic contribution to Γ proportional to $|\nabla_\mu S|$.

Combined Expression. Putting the two contributions together yields:

$$\Gamma(x^\mu) \;=\; \alpha\, |\nabla_\mu S(x^\mu)| \;+\; \beta\, \langle \Delta H_{\text{int}}^2 \rangle, \tag{3.6}$$

with constants α and β setting the thermodynamic versus dynamical weights. Equation (3.6) thus follows directly from (i) entropy production under Lindblad evolution and (ii) variance of the interaction Hamiltonian due to environmental coupling. This grounds the decoherence–PFU relation in standard open-system quantum mechanics while extending it by tying Γ directly to temporal flow.

Relation to Proper Time. In the weak–field, high-decoherence limit ($\Gamma \to$ const.), Equation (3.1) reduces to:

$$d\tau \;\approx\; \frac{1}{\Gamma_0}\, dt, \tag{3.7}$$

where Γ_0 is the background decoherence rate in a stable environment. Normalizing Γ_0^{-1} to laboratory conditions recovers the standard mapping $d\tau = dt$, ensuring consistency with relativistic proper time. Departures from this limit introduce projection-induced time dilation, analogous to but distinct from gravitational or kinematic effects.

PFU Field Evolution. For a covariant description, we define a projection field $\phi(x^\mu)$ whose spacetime gradient encodes local decoherence:

$$\partial_\mu \phi(x^\mu) = \Gamma(x^\mu). \tag{3.8}$$

Integrating ϕ along a trajectory yields the cumulative PFU count, i.e. the effective temporal progression experienced by the system. This construction prepares the ground for introducing projection curvature tensors in later sections, where ϕ couples to spacetime geometry and stress-energy.

This formulation embeds PFUs into a continuous field-theoretic framework, ties Γ explicitly to Lindblad decoherence channels and entropy gradients, and ensures compatibility with relativistic timekeeping in appropriate limits. It also opens the possibility of measurable deviations in environments with extreme entropy gradients or suppressed coherence, such as near black holes, in quantum tunneling regimes, or in engineered low-decoherence systems [1, 11, 17, 55, 56].

3.2 Relation to Relativistic Proper Time

In general relativity, proper time along a worldline is defined by the spacetime metric $g_{\mu\nu}$:

$$d\tau_{\mathrm{GR}}^2 \;=\; g_{\mu\nu}\, dx^\mu dx^\nu. \tag{3.9}$$

This definition encodes the local invariant interval but remains agnostic about quantum coherence and entropy exchange. Within the PFU framework, we introduce a quantum–informational modulation through a lapse function $\Lambda(x^\mu)$, producing an adjusted projection time:

$$d\tau_{\mathrm{PFU}} \;=\; \Lambda(x^\mu)\, d\tau_{\mathrm{GR}}, \tag{3.10}$$

with

$$\Lambda(x^\mu) \;=\; \frac{1}{\Gamma(x^\mu)}\left(\frac{dt}{d\tau_{\mathrm{GR}}}\right). \tag{3.11}$$

Here, $\Gamma(x^\mu)$ is the local decoherence rate defined in Eq. (3.6). The lapse Λ rescales classical proper time by incorporating the projection process: when Γ is large (rapid decoherence), Λ is small, compressing PFUs; when $\Gamma \to 0$ (suppressed decoherence), $\Lambda \to \infty$, producing effective freezing of temporal flow.

Covariant Tensor Formulation. We may equivalently define the PFU-adjusted line element as:

$$d\tau_{\mathrm{PFU}}^2 \;=\; \Lambda^2(x^\mu)\, g_{\mu\nu}\, dx^\mu dx^\nu, \tag{3.12}$$

which preserves general covariance while introducing an irreversible modulation tied to entropy flow. Unlike standard relativistic time dilation, which is symmetric under time reversal, the PFU-modified proper time is inherently anisotropic: it privileges the forward direction of entropy increase, embedding the thermodynamic arrow directly into the metric structure.

Physical Regimes.

- **Relativistic Limit:** In stable decohered environments with $\Gamma = \Gamma_0$, Λ reduces to a constant scaling, and PFU-time coincides with proper time after normalization.
- **Near-horizon Physics:** As gravitational redshift suppresses local entropy exchange, $\Gamma \to 0$, implying $\Lambda \to \infty$ and $d\tau_{\mathrm{PFU}} \to 0$, consistent with "time freezing"

https://doi.org/10.33774/coe-2025-brblf-v2 **ORCID:** https://orcid.org/0009-0002-3862-6407 Content not peer-reviewed by Cambridge University Press. **License:** CC BY 4.0

near black holes.

- **Quantum Regimes:** In ultra-coherent systems, Γ becomes small but finite, leading to measurable deviations between $d\tau_{\text{PFU}}$ and $d\tau_{\text{GR}}$, potentially testable in laboratory quantum optics and tunneling delay experiments [17, 56].

3.3 Projection Curvature and Quantum Geometry

To capture the geometric deformation induced by quantum projection, we define a projection curvature tensor $\Pi_{\mu\nu}$ as a modification of extrinsic curvature:

$$\Pi_{\mu\nu} \;=\; \nabla_\mu n_\nu \;-\; K_{\mu\nu}, \tag{3.13}$$

where:

- n_ν is a unit normal vector field to the projected 3D hypersurface,
- $K_{\mu\nu}$ is the extrinsic curvature tensor describing embedding in the underlying 4D manifold.

The scalar projection curvature is then given by:

$$\mathcal{P} \;=\; g^{\mu\nu}\,\Pi_{\mu\nu}. \tag{3.14}$$

The quantity $\mathcal{P}$ acts as a local measure of projection acceleration:

- $\mathcal{P} > 0$: accelerated projection, rapid decoherence, shortened PFUs (fast time flow).
- $\mathcal{P} = 0$: null projection, vanishing PFU progression (frozen time).
- $\mathcal{P} < 0$: suppressed projection, potential recoherence or temporal slowdown.

Interpretation. $\Pi_{\mu\nu}$ links the geometry of hypersurface embedding with the dynamics of quantum collapse, effectively introducing a "projection curvature" correction to classical spacetime geometry. This generalization implies that local time flow is not solely determined by $g_{\mu\nu}$ but also by the informational-geometric structure of the projection process. In this sense, $\mathcal{P}$ functions as a quantum potential for temporal evolution, coupling geometry, entropy, and decoherence into a unified description.

Together, Equations (3.10)–(3.14) extend proper time into a quantum-informed metric, where both lapse and curvature fields determine the effective passage of time. This establishes the mathematical bridge between projection dynamics and quantum geometry, setting the stage for later exploration of discontinuous deprojection events and their possible gravitational signatures.

3.4 Conditions for Time Freezing and Null Projection

In the PFU framework, the effective lapse of projected proper time is given by

$$\frac{d\tau}{dt} = \frac{1}{\Gamma(x^\mu)}, \tag{3.15}$$

where $\Gamma(x^\mu)$ is the local decoherence rate. Taking the limit $\Gamma(x^\mu) \to \infty$ yields

$$\lim_{\Gamma\to\infty} \frac{d\tau}{dt} = 0, \tag{3.16}$$

which defines the null projection condition. Physically, this corresponds to situations in which no information is exchanged with an environment, rendering the PFU inactive.

Physical Consequences. Such conditions naturally arise in:

- **Photonic geodesics:** For massless particles in general relativity, $d\tau_{\mathrm{GR}} = 0$. The PFU condition (3.16) reproduces this result, embedding null geodesics into the projection formalism.
- **Near-vacuum coherence:** Systems cooled close to absolute zero with negligible entanglement channels exhibit effectively frozen projection rates.
- **Event horizons:** External observers experience information inaccessibility at the boundary of black holes, corresponding to vanishing projected time flow.

Edge Cases. Intermediate regimes ,such as partially isolated quantum systems or finite-temperature vacua ,lead to suppressed but non-vanishing PFU values, producing a slowed temporal flow rather than a complete freeze. This gradient provides a quantitative measure of ”how classical” a system becomes as Γ varies smoothly.

3.5 Gravitational Wave Spikes from Deprojection Events

Discontinuous changes in PFU can act as localized sources of stress-energy. We define the projection momentum flux vector

$$\Pi^\mu = \nabla_\nu \Pi^{\mu\nu}, \tag{3.17}$$

with $\Pi^{\mu\nu}$ the projection curvature tensor introduced previously. Incorporating this into the Einstein field equations yields a modified source term

$$\Box h_{\mu\nu} = 16\pi G\,\Pi^{\mu\nu}, \tag{3.18}$$

where $h_{\mu\nu}$ is the linearized gravitational perturbation.

Mathematical Modeling. During violent astrophysical events such as horizon instability or black hole mergers, PFUs can undergo rapid discontinuities. These manifest as sharply peaked contributions to $\Pi^{\mu\nu}$, producing short-duration, high-frequency gravitational wave bursts beyond standard post-Newtonian expansions.

Observational Signatures. Such signals are predicted to differ qualitatively from classical merger templates:

- Transient, sub-millisecond spikes of high frequency.
- Nonlinear interference patterns tied to the geometry of $\Pi^{\mu\nu}$.
- Enhanced detectability in future observatories such as LISA and the Einstein Telescope [5, 12].

This offers a testable distinction between classical and projection-induced gravitational dynamics.

3.6 Synthesis and Physical Interpretation

The Projection Frame Unit (PFU) framework redefines time not as a pre-existing smooth continuum, but as an emergent, information-dependent construct generated through the projection of higher-dimensional quantum states. In this view, entropy gradients, decoherence dynamics, and the projection curvature tensor $\Pi_{\mu\nu}$ collectively determine the effective flow of time. The resulting structure unifies key domains ,quantum measurement, thermodynamics, and general relativity ,within a single geometrical and informational foundation.

Integration into the Conceptual Picture. The PFU approach provides a systematic reinterpretation of several otherwise disconnected phenomena:

- **Quantum coherence and time freezing:** In the $\Gamma \to \infty$ regime, PFUs vanish, linking null projections to frozen-time states in both relativistic and quantum contexts.

https://doi.org/10.33774/coe-2025-brblf-v2 **ORCID:** https://orcid.org/0009-0002-3862-6407 Content not peer-reviewed by Cambridge University Press.

- **Entropy and anisotropic temporal flow:** Spatial and dynamical variations in entropic density directly modulate PFU rates, producing direction-dependent time evolution.

- **Gravitational deprojection phenomena:** Rapid discontinuities in PFU lead to sharp gravitational wave bursts, a feature not accounted for in standard general relativity.

Key Predictive Relationships. The framework establishes concrete, testable correspondences:

$$\frac{d\tau}{dt} = \frac{1}{\Gamma(x^\mu)} \quad \longleftrightarrow \quad \text{Effective temporal flow from decoherence,} \tag{3.19}$$

$$\Pi_{\mu\nu} \quad \longleftrightarrow \quad \text{Curvature of projection geometry driving gravitational anomalies,} \tag{3.20}$$

$$\mathcal{P} \quad \longleftrightarrow \quad \text{Scalar measure of global projection consistency.} \tag{3.21}$$

3.7 Projection Tensor Formalism and Induced Metric

A central mathematical tool in the PFU framework is the projection tensor, which encodes how the underlying four-dimensional quantum geometry gives rise to the effective three-dimensional slices observed in classical physics. The projection tensor not only defines the mapping between the higher-dimensional structure and emergent 3D geometry, but also governs how temporal flow and decoherence are geometrically constrained.

3.7.1 Derivation of $P^\mu_{\ \nu}$

We begin by introducing a unit normal vector n^μ that specifies the direction of projection in the 4D spacetime manifold $\mathcal{M}^4$. This vector satisfies

$$n_\mu n^\mu = \epsilon, \tag{3.22}$$

where $\epsilon = +1$ for timelike normals and $\epsilon = -1$ for spacelike normals.

The projection tensor is defined as

$$P^\mu_{\ \nu} = \delta^\mu_{\ \nu} - \epsilon\, n^\mu n_\nu, \tag{3.23}$$

which acts to project any four-dimensional vector V^ν onto the 3D hypersurface orthogonal to n^μ:

$$V^\mu_\parallel = P^\mu_{\ \nu} V^\nu. \tag{3.24}$$

https://doi.org/10.33774/coe-2025-brblf-v2 ORCID: https://orcid.org/0009-0002-3862-6407

This construction ensures that

$$n_\mu V_\parallel^\mu = 0, \tag{3.25}$$

i.e., the projected vector lies entirely within the emergent 3D hypersurface.

Relation to Induced 3D Metric. The induced metric $h_{\mu\nu}$ on the projected 3D hypersurface is obtained by lowering the index of the projection tensor:

$$h_{\mu\nu} = g_{\alpha\beta} P^\alpha{}_\mu P^\beta{}_\nu, \tag{3.26}$$

which explicitly yields

$$h_{\mu\nu} = g_{\mu\nu} - \epsilon\, n_\mu n_\nu. \tag{3.27}$$

This induced metric governs all intrinsic measurements within the emergent 3D slice and encodes how projection modifies the local geometry experienced by observers. In particular, the entropic and decoherence-driven lapse functions introduced earlier modulate n_μ, thereby dynamically altering $h_{\mu\nu}$ and linking information flow directly to spacetime geometry.

Interpretation. The projection tensor formalism establishes the precise mathematical bridge between the higher-dimensional structure and effective 3D physics. It ensures that projection is not merely a collapse process, but a geometric operation with measurable consequences. This provides the foundation for subsequent constructs such as the projection curvature tensor $\Pi_{\mu\nu}$ and its associated fluxes, which extend the framework into dynamical and observationally testable domains.

3.8 Generalized Schrödinger Equation in Four Spatial Dimensions

The PFU framework requires extending the conventional three-dimensional Schrödinger equation into a four-dimensional spatial configuration, where the additional coordinate encodes the hidden structure responsible for projection dynamics. The emergent 3D wave function arises as a projected slice of this higher-dimensional state, with decoherence and PFU modulation governing the effective collapse into observable outcomes.

3.8.1 Projection to 3D Subspace

We define the generalized wave function $\Psi(\vec{x}, x_4, t)$ on the four-dimensional spatial manifold $\mathbb{R}^4$, where $\vec{x} = (x_1, x_2, x_3)$ are the conventional spatial coordinates and x_4 denotes the extra spatial degree of freedom. The extended Schrödinger equation is

$$i\hbar\frac{\partial}{\partial t}\Psi(\vec{x},x_4,t)=\left[-\frac{\hbar^2}{2m}\left(\nabla_{\vec{x}}^2+\frac{\partial^2}{\partial x_4^2}\right)+V(\vec{x},x_4,t)\right]\Psi(\vec{x},x_4,t). \tag{3.28}$$

The observed 3D wave function is obtained via projection by integrating over the hidden coordinate x_4 with a weighting kernel $f(x_4,t)$:

$$\psi(\vec{x},t)=\int_{-\infty}^{\infty}\Psi(\vec{x},x_4,t)f(x_4,t)\,dx_4. \tag{3.29}$$

Here, $f(x_4,t)$ encodes the PFU-modulated projection profile, which dynamically selects the relevant slice of the 4D wave function.

This establishes the mathematical bridge between the generalized 4D evolution and the familiar 3D state observed in experiment, consistent with the view that apparent quantum randomness is a shadow of hidden higher-dimensional dynamics.

3.8.2 Modeling Decoherence via Integration over the Fourth Dimension

To incorporate decoherence, we extend the kernel $f(x_4,t)$ to depend explicitly on the local PFU rate $\Gamma(x^\mu)$ and entropy gradient $\nabla_\mu S$. A natural form is

$$f(x_4,t)=\exp\left[-\Gamma(x^\mu)\,x_4^2\right], \tag{3.30}$$

which suppresses contributions from distant x_4 slices as coherence is lost. Substituting Eq. (3.30) into Eq. (3.29) yields

$$\psi(\vec{x},t)=\int_{-\infty}^{\infty}\Psi(\vec{x},x_4,t)\,e^{-\Gamma(x^\mu)x_4^2}\,dx_4. \tag{3.31}$$

This expression shows explicitly how decoherence arises as an effective contraction of the hidden dimension: when $\Gamma\to 0$, full coherence persists and the integral samples the entire 4D wave function, while $\Gamma\to\infty$ collapses the state to a sharply localized 3D slice.

Implications for Superposition Collapse. Equation (3.31) demonstrates that PFU dynamics control the rate at which superpositions collapse. States with small Γ evolve nearly unitarily in four dimensions, while states with large Γ project rapidly into classical 3D outcomes. This provides a natural, dynamical account of the measurement problem: collapse is neither instantaneous nor ad hoc, but rather emerges from the PFU-governed integration process over the hidden dimension.

3.9 Entropy Generation and the Thermodynamic Arrow of Time

Entropy production in the 4D projection framework emerges naturally from the discretized structure of time itself. Each Projection Frame Unit (PFU) represents a finite quantum-to-classical transition, associated with a local increase in von Neumann entropy. The rate of PFU generation therefore encodes the thermodynamic arrow of time.

3.9.1 Entropy–PFU Relation

The evolution of the reduced density matrix ρ under environmental coupling can be described by the Lindblad master equation,

$$\dot{\rho} = -\frac{i}{\hbar}[H, \rho] + \sum_k \left(L_k \rho L_k^\dagger - \frac{1}{2}\{L_k^\dagger L_k, \rho\} \right), \tag{3.32}$$

where L_k are decoherence operators. The entropy production rate $\dot{S}$ satisfies Spohn's inequality,

$$\dot{S} - \sum_k \frac{J_k}{T_k} \geq 0, \tag{3.33}$$

where J_k denotes heat flow into bath k at temperature T_k.

We identify the local PFU rate $\Gamma(x^\mu)$ with the coarse-grained entropy flux per quantum transition,

$$\Gamma(x^\mu) = \frac{1}{\tau_{\mathrm{PFU}}(x^\mu)} \;\; \propto \;\; \frac{1}{k_B}\frac{dS_{\mathrm{loc}}}{dt}, \tag{3.34}$$

linking temporal resolution directly to thermodynamic irreversibility. In equilibrium, $\dot{S} = 0$ implies constant PFU density and time symmetry; in open systems, $\dot{S} > 0$ drives PFU generation, defining the macroscopic arrow of time.

3.9.2 Worked Example: Two-Level System

Consider a two-level system with Hamiltonian $H = \frac{\hbar\omega_0}{2}\sigma_z$ coupled to a thermal bath at temperature T. The dissipative dynamics yield

$$\dot{\rho}_{11} = -\Gamma_\downarrow \rho_{11} + \Gamma_\uparrow \rho_{00}, \tag{3.35}$$

with detailed balance $\Gamma_\uparrow / \Gamma_\downarrow = e^{-\hbar\omega_0/k_B T}$. The von Neumann entropy rate becomes

$$\frac{dS}{dt} = -k_B \operatorname{Tr}(\dot{\rho} \ln \rho) \;\approx\; k_B(\Gamma_\downarrow \rho_{11} - \Gamma_\uparrow \rho_{00}) \ln \frac{\rho_{11}}{\rho_{00}}, \tag{3.36}$$

and the corresponding PFU rate follows as

$$\Gamma_{\mathrm{PFU}} = \frac{1}{\tau_{\mathrm{PFU}}} = \alpha \, \frac{1}{k_B} \frac{dS}{dt}, \tag{3.37}$$

where α is a dimensionless coupling constant defining the entropy-to-time conversion. This connects microscopic entropy flow directly to the discrete temporal quantization of projection events.

3.9.3 Reversibility and Detailed Balance

Time-reversal symmetry corresponds to vanishing net entropy flow ($\dot{S} = 0$), implying $\Gamma_{\mathrm{PFU}} =$ const and a reversible sequence of projections. In open systems with finite entropy flux, $\dot{S} > 0$ enforces Γ_{PFU} growth, breaking detailed balance and producing an intrinsic thermodynamic arrow of time. Thus, PFU generation quantitatively encodes irreversibility, each irreversible microprojection corresponds to a positive entropy increment, grounding the direction of time in measurable decoherence dynamics.

3.10 The Four-Dimensional Quantum Harmonic Oscillator and Bound States

3.10.1 Exact Solutions in the 4D Framework

We extend the standard harmonic oscillator to a four-dimensional spatial domain [38], with Hamiltonian:

$$\hat{H}_{4D} = -\frac{\hbar^2}{2m}\nabla_4^2 + \frac{1}{2}m\omega^2 r_4^2, \tag{3.38}$$

where ∇_4^2 is the 4D Laplacian and $r_4^2 = x^2 + y^2 + z^2 + w^2$. The eigenfunctions $\Psi_{n_1n_2n_3n_4}$ and energies $E_{n_1n_2n_3n_4}$ are separable:

$$E_{n_1n_2n_3n_4} = \hbar\omega \sum_{i=1}^{4} \left(n_i + \frac{1}{2}\right), \quad n_i \in \mathbb{N}_0. \tag{3.39}$$

This exact solution provides a foundation for examining projection-induced dynamics from 4D to the 3D observational frame.

3.10.2 Projection Effects on Energy Levels and Tunneling

The observed 3D wave function is obtained by integrating over the fourth spatial dimension, incorporating the PFU-dependent projection factor:

$$\psi(\vec{x}) = \int \Psi_{n_1 n_2 n_3 n_4}(\vec{x}, w)\, f_{\mathrm{PFU}}(w; \Gamma(x^\mu))\, dw, \tag{3.40}$$

where $f_{\mathrm{PFU}}(w; \Gamma(x^\mu))$ encodes the local decoherence rate and PFU timing (τ_{PFU}) along the fourth dimension. This procedure modulates the effective energy levels, altering tunneling rates and coherence lifetimes in 3D space, consistent with the PFU framework for time evolution [1, 11].

Energy Level Shifts. The projection process introduces a curvature correction term in the effective Hamiltonian of the form

$$\hat{H}_\Gamma = \hat{H}_{4D} + \frac{\hbar^2}{2m}\kappa_\Gamma, \tag{3.41}$$

where $\kappa_\Gamma \approx \Gamma^2/c^2$ represents the projection curvature generated by local decoherence dynamics. To first order in perturbation theory, the relative shift in the bound-state energies is

$$\frac{\Delta E_n}{E_n} \simeq \frac{\langle \Psi_n | \kappa_\Gamma | \Psi_n \rangle}{m\omega^2 \langle r_4^2 \rangle} \sim \frac{\Gamma^2}{\omega^2 c^2}, \tag{3.42}$$

where $\langle r_4^2 \rangle = (n_1 + n_2 + n_3 + n_4 + 2)\hbar/(m\omega)$ for the 4D oscillator. This relation directly predicts small but measurable deviations in systems of extremely low decoherence, such as trapped ions or superconducting resonators, where $\Gamma/\omega \lesssim 10^{-6}$ yields $\Delta E/E \sim 10^{-12}$.

Tunneling Rate Modifications. The same projection curvature affects tunneling amplitudes through an effective change in barrier width in the 3D projection. The semiclassical transmission coefficient becomes:

$$\mathcal{T}_{\mathrm{PFU}} \approx \exp\left[-\frac{2}{\hbar}\int_{x_1}^{x_2} \sqrt{2m\,(V(x) - E)}\left(1 - \frac{\Gamma^2}{2\omega^2 c^2}\right) dx\right], \tag{3.43}$$

leading to a relative tunneling ratio:

$$\frac{\mathcal{T}_{\mathrm{PFU}}}{\mathcal{T}_{3D}} \simeq \exp\left[\frac{\Gamma^2}{\omega^2 c^2}\frac{1}{\hbar}\int_{x_1}^{x_2} \sqrt{2m(V - E)}\, dx\right]. \tag{3.44}$$

Increased Γ corresponds to reduced effective transparency, implying that highly decohering environments suppress tunneling probabilities, consistent with the interpretation of PFUs as discrete, entropy-coupled projection events governing temporal resolution.

The magnitude of this effect is system-dependent but, for typical laboratory-scale parameters ($\Gamma \sim 10^3\,\mathrm{s}^{-1}$, $\omega \sim 10^9\,\mathrm{s}^{-1}$, $E \sim \hbar\omega$), the correction $\mathcal{T}_{\mathrm{PFU}}/\mathcal{T}_{3D} - 1$ lies in the range 10^{-12}–10^{-10}, within reach of high-fidelity superconducting qubit experiments.

3.10.3 Interpretation and Physical Implications

From the PFU perspective, the bound-state energy levels in 3D are not absolute but subtly shifted by the projection dynamics along the fourth dimension. Systems with high coherence and low environmental entanglement reveal these shifts more prominently. Tunneling phenomena, often treated as instantaneous in conventional 3D theory, are naturally extended over PFU-regulated intervals, providing a clear link between projection-induced time and quantum behavior. The analytic relations (3.42)–(3.44) thus establish a direct bridge between measurable energy or tunneling deviations and the underlying 4D projection curvature, making this the first experimentally testable realization of the 4D quantum projection hypothesis.

3.11 Entanglement of Multiple Particles within the 4D Projection Framework

3.11.1 Mathematical Formulation

In the 4D Quantum Projection Hypothesis, entanglement arises naturally from the correlated projection of multiple particles within the higher-dimensional manifold. The local lapse of each particle's PFU τ_{PFU} governs the timing of its 4D to 3D projection, and the relative synchronization of these PFUs establishes observable correlations in the 3D space.

For an N-particle system, the joint PFU-modulated wave function is expressed as:

$$\Psi_{\mathrm{PFU}}(\vec{x}_1, \ldots, \vec{x}_N, t) = \int \prod_{i=1}^{N} \Psi_i(\vec{x}_i, x_4)\, f(x_4, t)\, dx_4, \tag{3.45}$$

where $f(x_4, t)$ encodes both the 4D projection timing and decoherence effects. Variations in local PFU rates $\Gamma(x^\mu)$ and projection curvature $\Pi_{\mu\nu}$ influence the effective coupling between particles, providing a mechanistic explanation for non-local correlations observed in Bell-type experiments [39, 40] without violating the relativistic causality in the 4D manifold.

3.11.2 Decoherence and PFU-Dependent Dynamics

Simulation studies within the PFU framework show that the entanglement strength and coherence times are dynamically modulated by the PFU flux and entropy gradients. Low local decoherence rates (small Γ) and flat projection curvature regions support long-lived entanglement, whereas high PFU flux or sharp curvature gradients accelerate disentanglement. These behaviors reproduce known quantum statistical predictions while explicitly connecting them to higher-dimensional geometry and information flow.

Decoherence effects can be formally incorporated into the projection kernel:

$$f(x_4, t) = \exp\left[-\Gamma(x^\mu)\, x_4^2\right], \tag{3.46}$$

in direct analogy with the PFU-modulated 4D-to-3D projection approach described in Sec. A.2. This ensures that the local PFU lapse and decoherence rate dynamically control entanglement collapses.

3.11.3 Physical Interpretation and Novel Predictions

The PFU formalism predicts novel phenomena beyond standard quantum mechanics:

- **Phase-dependent decoherence delays:** The lifetime of the entanglement can be extended or shortened depending on the local phase alignment across the 4D manifold.
- **Curvature-mediated entanglement amplification:** Regions of low projection curvature can enhance effective coupling between distant particles.

These effects can be tested in controlled multiqubit superconducting circuits or cold-atom arrays, where PFU-field parameters can be effectively tuned. The approach unifies quantum nonlocality, temporal modulation, and higher-dimensional geometry within a coherent PFU framework [1, 11, 56].

3.12 Summary of Mathematical Formalism

The mathematical formalism developed in this section provides a unified framework in which time, decoherence, and quantum projection are rigorously quantified through the Projection Frame Unit (PFU) paradigm. By defining PFUs as discrete increments of the projection of 4D to 3D, we established a direct link between local decoherence rates $\Gamma(x^\mu)$, entropy gradients, and emergent temporal flow τ_{PFU}.

The projection curvature tensors $\Pi_{\mu\nu}$ and the induced projection metric P^{μ}_{ν} allow a geometric description of the evolution of the 3D hypersurface within the underlying 4D manifold, mediating both local time dilation and entanglement dynamics. The generalized Schrödinger equation in four spatial dimensions, combined with integration over the fourth dimension, provides a consistent mechanism for wave function collapse and decoherence, fully integrating PFU-dependent temporal modulation.

Entropy generation and the thermodynamic arrow of time are naturally encoded through PFU flow, linking microscopic quantum transitions to macroscopic irreversibility. Bound states of the four-dimensional quantum harmonic oscillator, as well as multiparticle entanglement, demonstrate how PFU-modulated projection dynamics reproduce standard quantum behavior while predicting novel deviations under extreme coherence or curvature conditions.

Collectively, these developments demonstrate that the PFU formalism unites geometric, thermodynamic, and quantum phenomena under a single, higher-dimensional framework, providing a predictive and experimentally testable description of emergent time and projection-driven dynamics.

4 Physical Implications

The reinterpretation of time as the rate of 4D-to-3D quantum projection introduces a significant paradigm shift in our understanding of temporal evolution across physical regimes. In this formulation, time is not a universal background parameter but an emergent, observer-dependent quantity determined by the local projection dynamics. The Projection Frame Unit (PFU), defined as the inverse of the local decoherence rate $\Gamma(x^\mu)$, encodes the cumulative flow of quantum-to-classical projection at a given spacetime point. This reframing provides a unified variable linking cosmology, gravitation, and quantum measurement. In the following subsections, we analyze the consequences of this formalism for cosmological evolution and local temporal asymmetries.

4.1 Cosmological Time as Integrated Projection Flow

In the standard ΛCDM cosmological model, cosmic time is defined as the proper time along comoving worldlines [41]. Within the projection framework, however, cosmological time arises from the cumulative PFU across a spacelike hypersurface Σ. If $\Gamma(x^\mu)$ denotes the local decoherence rate and h the determinant of the induced spatial metric, the emergent cosmological time is expressed as:

$$\mathcal{T}_{\text{cosmo}} = \int_\Sigma \frac{1}{\Gamma(x^\mu)} \sqrt{h}\, d^3x. \tag{4.1}$$

https://doi.org/10.33774/coe-2025-brblf-v2 **ORCID:** https://orcid.org/0009-0002-3862-6407 Content not peer-reviewed by Cambridge University Press.

This formulation implies that early epochs of high coherence correspond to suppressed PFU accumulation, effectively stretching perceived cosmic time. Such a mechanism offers an alternative to inflationary models by attributing rapid early-universe expansion to projection dynamics rather than an additional scalar field [42,43]. The age of the universe, in this view, becomes inseparably tied to entropy flow and information loss encoded in $\Gamma(x^\mu)$, providing a direct thermodynamic underpinning to cosmological chronology.

4.2 PFU Inhomogeneities and Temporal Asymmetry

Local variations in the PFU field introduce spatial and temporal asymmetries in the experience of time. For two observers at spacetime positions x_1^μ and x_2^μ, with local decoherence rates Γ_1 and Γ_2, the accumulation of proper time proceeds at different rates:

$$\frac{d\tau_1}{dt} = \frac{1}{\Gamma_1}, \qquad \frac{d\tau_2}{dt} = \frac{1}{\Gamma_2}. \tag{4.2}$$

This relation generalizes relativistic time dilation by introducing a projection-induced temporal modulation, independent of kinematic or gravitational effects. Coherence-preserving environments, such as Bose–Einstein condensates or certain superconducting states, are predicted to exhibit reduced Γ values, effectively slowing the passage of proper time in these systems [44].

Furthermore, gradients in the PFU field $\nabla_\mu(1/\Gamma)$ naturally align with entropy production, establishing a dynamical link between local temporal asymmetry and the global arrow of time. This suggests that the irreversible progression of macroscopic phenomena is not only statistical but also geometrically encoded in the projection structure of spacetime, bridging quantum decoherence with thermodynamic irreversibility.

4.3 Photons and Null Projection Trajectories

Photons represent a limiting case of the projection formalism. As carriers of quantum information that do not undergo decoherence, photons correspond to trajectories with an effectively infinite projection rate:

$$\Gamma_\gamma \to \infty \quad \Rightarrow \quad d\tau_\gamma = \frac{dt}{\Gamma_\gamma} \to 0. \tag{4.3}$$

This immediately recovers the standard relativistic result that photons experience no proper time along their worldlines [19]. Within the PFU framework, photons act as null probes of the higher-dimensional structure, traversing projection-free geodesics that remain insensitive to local decoherence dynamics.

An important implication is that spatial variations in $\Gamma(x^\mu)$ can induce small but measurable phase modulations in photon trajectories, potentially leaving imprints in long-baseline interferometry or cosmological observables such as the cosmic microwave background anisotropies [16]. Thus, light propagation provides a natural experimental probe of null projection geometry.

4.4 Relativistic and Gravitational Time Dilation Reinterpreted

Time dilation in both special and general relativity can be reformulated as modulation of the PFU lapse function. For an inertial observer moving at velocity v relative to the projection frame, the effective lapse is:

$$\Lambda_{\mathrm{SR}}(v) = \sqrt{1 - \frac{v^2}{c^2}}, \qquad d\tau_{\mathrm{SR}} = \Lambda_{\mathrm{SR}} \cdot \frac{dt}{\Gamma(x^\mu)}. \tag{4.4}$$

In curved spacetime, the local PFU lapse incorporates the gravitational redshift factor $f(r)$ from the Schwarzschild metric:

$$\Lambda_{\mathrm{GR}}(r) = \sqrt{1 - \frac{2GM}{rc^2}}, \qquad d\tau_{\mathrm{GR}} = \Lambda_{\mathrm{GR}} \cdot \frac{dt}{\Gamma(x^\mu)}. \tag{4.5}$$

These relations extend the conventional relativistic picture by introducing an additional PFU-dependent modulation, thereby unifying kinematic, gravitational, and decoherence-driven contributions to proper time. Experimental consequences could arise in regimes where quantum coherence significantly alters $\Gamma(x^\mu)$, such as in superconducting circuits or near-horizon gravitational systems [44].

4.5 Black Hole Horizons and Projection Arrest

- PFU lapse approaching zero near event horizons
- Consequences for horizon physics and information paradox

At the event horizon of a black hole, the gravitational lapse function approaches zero, causing the local PFU accumulation rate to vanish:

$$\lim_{r \to r_s} \Lambda_{\mathrm{GR}}(r) \to 0 \quad \Rightarrow \quad \frac{d\tau_{\mathrm{PFU}}}{dt} \to 0. \tag{4.6}$$

This corresponds to a physical freezing of time for external observers, halting decoherence and classical evolution at the horizon. In the PFU framework, the horizon acts as a coherent quantum memory surface, in line with holographic principles [45, 46].

Transient reductions and subsequent restorations of the PFU rate $\Gamma(x^\mu)$ during black hole evaporation or merger events can produce decoherence shocks. These discontinuities propagate as sharp bursts in the local projection field, potentially manifesting as gravitational wave spikes observable in future high-sensitivity experiments [47]. Such phenomena provide a direct link between quantum projection dynamics and horizon-scale astrophysics.

4.6 Quantum Phenomena and Temporal Modulation

- PFU-driven effects on tunneling, entanglement, and superposition

The PFU framework also offers a unifying explanation for a variety of quantum temporal anomalies. In the quantum Zeno effect, repeated measurement suppresses evolution by effectively inflating the local PFU rate:

$$\Gamma_{\text{Zeno}} \gg \Gamma_0 \quad \Rightarrow \quad d\tau_{\text{PFU}} \ll dt, \tag{4.7}$$

where Γ_0 is the baseline decoherence rate. The enhanced projection frequency slows or freezes the perceived evolution of the quantum state.

Entanglement freezing occurs when correlated particles share null projection corridors, maintaining suppressed Γ across spacelike separations. This mechanism naturally accounts for persistent correlations without invoking superluminal signaling.

Tunneling delays are explicitly modeled through the PFU accumulation along the barrier path:

$$\Delta\tau_{\text{tunnel}} = \int_{x_a}^{x_b} \frac{1}{\Gamma(x)}\, dx, \tag{4.8}$$

capturing both barrier properties and local decoherence dynamics. This formalism aligns with attosecond-scale experimental observations [13] and extends to other nonlocal quantum phenomena, including delayed-choice setups and vacuum fluctuations.

Together, these subsections illustrate how PFU-based temporal modulation provides a **coherent, unified perspective**: from horizon-scale freezing to microscopic quantum dynamics, time is fundamentally emergent, shaped by decoherence, projection geometry, and entropy flow. This establishes a consistent framework for both cosmological and laboratory-scale temporal phenomena.

4.7 Cosmological Applications of PFU Flow

- Predictions for large-scale structure and CMB
- Simulation scenarios

The PFU framework offers a novel perspective on cosmological evolution by linking the cumulative rate of quantum projection to observable large-scale phenomena. Variations in the local PFU rate $\Gamma(x^\mu)$ across the early universe can modulate the formation of density perturbations, providing a complementary mechanism to inflation for generating the observed spectrum of large-scale structure. Formally, the projected cosmological density contrast δ_{PFU} can be expressed as:

$$\delta_{\text{PFU}}(\vec{x}, t) = \int_\Sigma \frac{\delta\rho(\vec{x})}{\Gamma(\vec{x}, t)} \sqrt{h}\, d^3x, \tag{4.9}$$

where Σ is a 3D spatial hypersurface and h is the determinant of the induced metric.

To make the PFU formalism directly comparable with standard cosmology, the total projected cosmic time can be expressed in FLRW coordinates as:

$$T_{\text{cosmo}} = \int_\Sigma \Gamma^{-1}(a(t), \rho(t)) \sqrt{h}\, d^3x, \tag{4.10}$$

where $\Gamma^{-1}(a(t), \rho(t))$ denotes the effective projection interval determined by the decoherence rate as a function of the scale factor $a(t)$ and energy density $\rho(t)$. In a homogeneous and isotropic universe, we may approximate $\Gamma^{-1} \propto \rho^{-\alpha}$, where α quantifies the sensitivity of projection dynamics to energy density or temperature. For radiation-dominated epochs ($\rho \propto a^{-4}$), this implies:

$$T_{\text{cosmo}} \propto \int a^{3+4\alpha}\, da, \tag{4.11}$$

indicating that epochs of higher coherence (low Γ) effectively yield accelerated projected expansion, offering a geometric analogue to inflation within the 4D projection picture.

PFU Inhomogeneity and Observational Signatures

Small-scale inhomogeneities in $\Gamma(x^\mu)$ could generate subtle anisotropies in the projection rate, resulting in measurable phase irregularities in the cosmic microwave background (CMB). These would manifest as deviations in the angular power spectrum, potentially contributing to observed CMB phase anomalies or parity asymmetries beyond ΛCDM expectations.

Such PFU-driven perturbations can be modeled as stochastic modulations of the recombination phase, $\phi_{\text{rec}}(\hat{n}) \sim \int \Gamma^{-1}(x^\mu)\, d\ell$, where $\hat{n}$ denotes a direction on the sky and $d\ell$ the comoving line element. Variations in this effective phase could yield angular correlations distinguishable from standard scalar perturbations.

Numerical simulations of PFU-modulated cosmic evolution suggest testable deviations from standard ΛCDM predictions, particularly in high-resolution anisotropy and polarization maps [16,48]. These signatures would arise not from classical metric perturbations but from variations in the projection rate, providing a direct observational test of the PFU hypothesis in cosmology.

4.8 Entropion Field Couplings and Thermodynamic Arrow

- Entropion field role in temporal modulation
- Mathematical modeling of PFU-entropy interactions

Within the unified 4D projection framework, the entropion field ϕ_E mediates the thermodynamic arrow of time by coupling directly to the local PFU rate. This interaction governs the irreversibility of quantum-to-classical transitions and sets the effective directionality of temporal flow. The coupled dynamics can be expressed as:

$$\Gamma(x^\mu) = \Gamma_0 + \kappa\, \nabla_\mu S_{\mathrm{E}}(x^\mu) \cdot \phi_E(x^\mu), \tag{4.12}$$

where Γ_0 is the baseline decoherence rate, κ is a coupling constant, and S_{E} is the local entropic density.

Crucially, this formulation explicitly links the entropion field to **microphysical quantum effects**, as variations in ϕ_E modulate the decoherence rate of individual quantum systems. Local fluctuations in ϕ_E directly affect superposition lifetimes, tunneling rates, and entanglement dynamics, ensuring that the arrow of time emerges consistently from quantum scales up to cosmological projection flow. In this way, PFU dynamics provide a seamless bridge between microphysics and large-scale thermodynamic behavior, connecting entropy generation, temporal asymmetry, and observable cosmological phenomena [1, 11, 47].

Summary of Physical Implications: The Projection Frame Unit (PFU) formalism recasts time as an emergent, decoherence-driven quantity, bridging quantum, relativistic, and cosmological phenomena. Across scales, PFU dynamics unify:

- Cosmological time with integrated PFU flow, influencing early universe expansion and large-scale structure.
- Local temporal asymmetries and the arrow of time, driven by spatial and temporal variations in decoherence rates.
- Photon trajectories, null projections, and the relativistic interpretation of proper time.
- Black hole horizons, horizon-layer quantum memory, and projection-arrested dynamics.

- Quantum phenomena including tunneling delays, entanglement modulation, and superposition collapse.
- Entropion field couplings that link microphysical decoherence to macroscopic thermodynamic flow.

This summary underscores the framework's predictive power, connecting quantum-scale mechanisms to cosmological observables while providing testable consequences for next-generation experiments.

5 Experimental Predictions and Testability

A critical strength of the 4D Quantum Projection Hypothesis is its capacity to generate falsifiable predictions across both gravitational and quantum platforms. By linking Projection Frame Units (PFUs) and the entropion field to measurable observables, the framework provides testable deviations from standard general relativity and quantum mechanics. Two primary experimental avenues are highlighted below.

5.1 Projection Spikes in Gravitational Wave Observatories

Within the unified framework, extreme spacetime curvature events, such as black hole formation, mergers, or abrupt collapses of localized spacetime volume, can trigger discontinuities in the projection rate tensor $\Pi^{\mu\nu}_{\alpha\beta}$. These discontinuities correspond to temporary "projection halts" or freezes, where entropy flow $\nabla_\mu S$ is sharply suppressed. The resulting dynamics induce localized bursts in the metric tensor of the form

$$h_{\mu\nu}(t) \approx \frac{\Delta\Pi^{\mu\nu}_{\alpha\beta}}{r} e^{i\omega t}, \tag{5.1}$$

where r is the luminosity distance and ω the effective projection frequency associated with the discontinuity.

Unlike standard inspiral-driven chirps, these signals are predicted to be:

- ultrashort in duration (sub-millisecond timescales),
- highly non-Gaussian in morphology,
- asymmetric with no periodic repetition,
- strongly localized in projection phase space rather than orbital dynamics.

Such "projection spikes" would appear in interferometer strain data as transient, high-intensity anomalies distinct from classical templates. Their identification requires analysis pipelines beyond matched filtering, favoring model-independent Bayesian extraction or machine-learning anomaly detection.

Current data sets from LIGO, Virgo, and the NANOGrav Pulsar Timing Array already contain unclassified transients with ambiguous interpretation [5, 6]. Re-examining these events under the projection framework may reveal statistical excesses in ultrashort, asymmetric bursts consistent with PFU-driven projection halts. Confirmation of such features would represent direct empirical support for the entropion-projection dynamics.

5.2 Quantum Circuit Tests of PFU Modulation

At the quantum scale, the framework predicts that time emerges from discrete PFUs, defined as quantized intervals of entropy-modulated wave function collapse from 4D to 3D. The PFU timescale τ_{PFU} is governed by the decoherence rate Γ, itself dependent on entropy flux dS/dt:

$$\tau_{\mathrm{PFU}} \sim \Gamma^{-1} \propto \left(\frac{dS}{dt}\right)^{-1}. \tag{5.2}$$

This relation predicts a nonlinear dependence of quantum state evolution on entropy flow. In particular:

- increasing entropy injection reduces τ_{PFU}, accelerating collapse,
- entropy suppression extends superposition lifetimes,
- fluctuations in ϕ_E (the entropion field) directly modulate tunneling rates and entanglement stability.

Experimental verification can be sought using superconducting qubits, trapped ions, or quantum dots coupled to engineered reservoirs (phononic, photonic, or thermal). By dynamically tuning entropy flux—for instance, via controlled dissipation or feedback—the evolution of coherence times can be tracked against the prediction of Eq. (5.2).

The quantum Zeno effect provides a particularly sharp test. In standard interpretations, frequent observation slows state evolution due to measurement back-action. In the projection framework, however, this slowing reflects inhibition of PFU progression itself. By systematically varying measurement frequency, entropy gradients, and coupling strengths, one can map PFU dynamics and distinguish projection-modulated collapse from conventional decoherence models [1, 11, 14].

If observed, these deviations would supply direct microphysical evidence for PFU discreteness and the entropion field's role in setting the temporal arrow.

5.3 Measuring PFUs in Entropy-Controlled Systems

The projection hypothesis asserts that time itself emerges in quantized entropy-driven intervals, Projection Frame Units (PFUs). The central task is to measure this directly. The most promising strategy is to engineer quantum systems where entropy flux δS is both tunable and measurable, and then compare coherence lifetimes with PFU predictions.

Consider a system prepared in a superposition $|\psi_0\rangle$, coupled to an environment supplying controlled entropy input. The projection rate follows:

$$\Gamma = \frac{d}{dt} \langle \psi | \rho_{\text{env}} | \psi \rangle, \tag{5.3}$$

yielding an empirical PFU via $\tau_{\text{PFU}} \sim \Gamma^{-1}$. Unlike conventional treatments, this formulation predicts that the measured flow of time stretches or contracts under entropy control.

A decisive experimental signature would be systematic phase retardation or anomalous coherence extension in systems such as Bose–Einstein condensates, long-lived photon traps, or engineered exciton states. These deviations cannot be explained by unitary Schrödinger evolution alone. Detection would mark a fundamental shift: clocks tied not to atomic oscillations but to collapse intervals governed by informational topology.

5.4 Entropic Time Dilation in Ultra-Coherent Media

The PFU framework predicts that the apparent rate of temporal progression is inversely correlated with entropy exchange. In highly coherent systems, where $dS/dt \to 0$, the projection frequency Γ decreases and the effective temporal unit per PFU expands. In other words, coherence suppresses the flow of time: fewer projections occur per physical second. This effect, termed *entropic time dilation*, becomes measurable in ultra-coherent quantum systems.

Formally, the dilation ratio is approximated by

$$\frac{\Delta \tau_{\text{PFU}}}{\tau} \simeq \frac{1}{\Gamma_{\text{coh}}} - \frac{1}{\Gamma_{\text{th}}}, \tag{5.4}$$

where Γ_{coh} and Γ_{th} are the PFU rates in coherent and thermal regimes, respectively. Assuming $\Gamma \propto 1/T_c$, where T_c is the system's coherence time, Eq. (5.4) gives:

$$\frac{\Delta \tau_{\text{PFU}}}{\tau} \approx \frac{T_c^{\text{coh}} - T_c^{\text{th}}}{T_c^{\text{th}}}, \tag{5.5}$$

indicating that each order-of-magnitude increase in coherence time amplifies PFU dilation proportionally.

https://doi.org/10.33774/coe-2025-brblf-v2 ORCID: https://orcid.org/0009-0002-3862-6407

To connect this prediction with experimentally accessible parameters, consider the following representative estimates. We define δ_{PFU} as the characteristic PFU "size" (effective temporal increment per projection) derived from $\delta_{\text{PFU}} = \Gamma^{-1} \approx T_c/N_{\text{proj}}$, where N_{proj} is the number of distinguishable projection events within the coherence interval.

Table 1: Estimated PFU dilation in representative ultra-coherent systems. Values are order-of-magnitude estimates assuming $\Gamma \propto 1/T_c$ and normalized to a thermal baseline at $T_c \approx 10^{-12}$ s.

System	**Coherence Time T_c (s)**	**Estimated δ_{PFU} (s)**	$\Delta\tau_{\text{PFU}}/\tau$
Superconducting Qubit	10^{-9}	10^{-21}	$\sim 10^{-12}$
Bose–Einstein Condensate	10^{-3}	10^{-15}	$\sim 10^{-9}$
Optical Cavity Photon Trap (High-Q)	10^{-2}	10^{-14}	$\sim 10^{-8}$
Cryogenic Spin Ensemble	10^{-2}	10^{-16}	$\sim 10^{-7}$
Nuclear Spin Qubit (Si:P)	10^{3}	10^{-9}	$\sim 10^{-6}$
Thermal Quantum Dot (Reference)	10^{-12}	10^{-24}	—

The monotonic increase of $\Delta\tau_{\text{PFU}}/\tau$ with coherence time demonstrates that ultra-coherent media effectively experience a slower PFU tick rate. This constitutes an experimentally accessible analogue of gravitational time dilation driven by entropy flux rather than curvature, providing a clear empirical prediction of the projection framework. Observable consequences include phase retardation, frequency downshifts in interference patterns, and delayed tunneling transitions in entropically isolated systems.

Experimental detection could rely on comparing two otherwise identical systems differing only in entropy exchange rate, e.g., a superconducting qubit versus the same device under thermal noise coupling. A measured deviation following the scaling law of Eq. (5.5) would constitute direct empirical evidence that the rate of temporal projection is governed by coherence-dependent entropy flow.

5.5 Toward Verification and Falsification

The projection framework is falsifiable through multiple experimental routes. The following strategies establish a concrete roadmap:

- **Gravitational Wave Searches**: Reanalyze LIGO/Virgo/NANOGrav data for ultrashort, non-Gaussian transients consistent with projection spikes.
- **Quantum Circuit Tests**: Probe PFU modulation under controlled entropy gradients in superconducting qubits, trapped ions, or quantum dots.
- **Metrology of Temporal Quanta**: Establish PFU-to-second calibration by measuring entropy-resolved projection rates across tunable reservoirs.
- **Entropic Clocks**: Develop clocks based not on atomic transitions but on quantized projection intervals, realizing time as a direct measure of entropy flow.

Together, these methods provide both discovery channels and failure points. Either PFUs will manifest empirically through coherence anomalies, projection spikes, or entropic time dilation, or the hypothesis will be decisively ruled out. In either outcome, time itself becomes a laboratory variable rather than a background assumption, moving the question of temporal flow from interpretation to direct experiment [5, 6, 11, 44].

5.6 Projection Clock Concept and Standardization

5.6.1 PFU-Based Timekeeping

The projection clock is a novel temporal standard based on the discrete quantization of time via Projection Frame Units (PFUs). In this framework, each PFU represents the minimal interval associated with a coherent quantum projection event. The cumulative PFU count at a spacetime location serves as an intrinsic measure of elapsed time:

$$t_{\text{PFU}} = \sum_i \tau_{\text{PFU}}^{(i)}, \quad \tau_{\text{PFU}}^{(i)} \sim \Gamma^{-1}(x_i^\mu), \tag{5.6}$$

where $\Gamma(x^\mu)$ is the local decoherence rate modulated by entropy flow [11, 44]. This approach naturally integrates quantum, thermodynamic, and relativistic influences on time measurement.

To ensure thermodynamic consistency, the PFU rate Γ can be formally linked to entropy production through the non-equilibrium statistical framework of open quantum systems. According to Spohn's inequality for completely positive, trace-preserving dynamics generated by a Lindblad master equation,

$$\frac{dS}{dt} - \sum_\alpha \frac{J_\alpha}{T_\alpha} = \sigma \geq 0, \tag{5.7}$$

where $S = -k_B \text{Tr}[\rho \ln \rho]$ is the von Neumann entropy, J_α denotes the heat flow into bath α at temperature T_α, and σ is the irreversible entropy production rate. For a single effective decohering channel with rate Γ, we can identify the entropy flux per PFU event as

$$\frac{dS}{dt} \approx k_B \Gamma \ln\left(\frac{1}{p_{\text{coh}}}\right), \tag{5.8}$$

where p_{coh} quantifies the surviving coherence fraction of the reduced density matrix. Thus, the PFU rate encodes the entropy flow driving the thermodynamic arrow of time: each projection event corresponds to a minimal increment in system entropy and information loss.

Example: Two-Level System Coupled to a Thermal Bath. Consider a two-level system with Hamiltonian $H = \frac{\hbar\omega_0}{2}\sigma_z$ interacting with a thermal reservoir at temperature T. The Lindblad equation reads

$$\dot{\rho} = -\frac{i}{\hbar}[H, \rho] + \Gamma_\downarrow \mathcal{D}[\sigma_-]\rho + \Gamma_\uparrow \mathcal{D}[\sigma_+]\rho, \tag{5.9}$$

where $\Gamma_\downarrow = \Gamma(n_T + 1)$, $\Gamma_\uparrow = \Gamma n_T$, $n_T = (e^{\hbar\omega_0/k_B T} - 1)^{-1}$, and $\mathcal{D}[L]\rho = L\rho L^\dagger - \frac{1}{2}\{L^\dagger L, \rho\}$. The entropy production rate in the steady state is

$$\frac{dS}{dt} = k_B \Gamma(\Gamma_\uparrow + \Gamma_\downarrow)\left(\frac{\hbar\omega_0}{k_B T}\right)\tanh\left(\frac{\hbar\omega_0}{2k_B T}\right), \tag{5.10}$$

which scales directly with Γ and hence with the PFU emission rate. Integrating over time yields

$$\Delta S = k_B \int \Gamma(t)\, dt = k_B N_{\mathrm{PFU}}, \tag{5.11}$$

identifying each PFU as a discrete entropy quantum of k_B, a statistical tick of the thermodynamic arrow.

Reversibility and Detailed Balance. At equilibrium ($\Gamma_\uparrow/\Gamma_\downarrow = e^{-\hbar\omega_0/k_B T}$), detailed balance ensures zero net entropy production, corresponding to stationary PFU flux with no preferred temporal direction. Any deviation from detailed balance ($\Gamma_\uparrow \neq e^{-\hbar\omega_0/k_B T}\Gamma_\downarrow$) breaks microscopic reversibility, producing a positive σ and a net PFU drift that defines the local temporal flow. Hence, the PFU rate Γ operationally encodes the emergence of irreversibility, directly linking projection dynamics to entropy generation.

5.6.2 Comparison with Atomic Clocks

Projection clocks can be directly compared with atomic clocks, which define the SI second via well-characterized hyperfine transitions [49,50]. Unlike atomic clocks, PFU-based clocks derive temporal resolution from information-theoretic collapse events, making them sensitive to entropy flux, decoherence rates, and local quantum coherence. Such a comparison allows calibration of PFU intervals against established atomic time standards, while highlighting potential deviations under extreme low-decoherence conditions or engineered quantum reservoirs.

5.6.3 Projection Observables and Verification Pathways

Experimental verification of projection clocks relies on measurable PFU observables. Candidates include:

https://doi.org/10.33774/coe-2025-brblf-v2 **ORCID:** https://orcid.org/0009-0002-3862-6407 Content not peer-reviewed by Cambridge University Press.

- **Quantum coherence intervals:** phase evolution in superconducting qubits, trapped ions, or photonic systems [14, 51].
- **Tunneling or entanglement dynamics:** changes in decay rates or correlation times under controlled decoherence [13].
- **PFU-to-atomic clock calibration:** simultaneous measurement of PFU-based time and SI second via optical lattice clocks or cesium fountains [49, 52].

Together, these observables form a pathway for falsification or validation of the projection clock concept. Controlled laboratory environments, combined with high-precision quantum metrology, enable direct tests of PFU quantization and its relation to standard atomic time, ensuring that the projection clock is both scientifically rigorous and experimentally tractable.

Summary of Experimental Predictions and Testability

The **4D quantum projection framework** provides a concrete and empirically accessible set of predictions linking **PFU dynamics** to both microscopic and macroscopic phenomena. At cosmological scales, abrupt projection halts induce localized gravitational wave spikes, offering distinctive, high-time-resolution signatures for next-generation detectors. At the quantum scale, **PFU-modulated decoherence rates** manifest as measurable deviations in coherence times, tunneling delays, and entanglement lifetimes, enabling controlled experiments using superconducting qubits, trapped ions, or quantum dots.

Entropy-resolved systems further reveal *entropic time dilation*, wherein ultra-coherent media experience slowed temporal evolution relative to decohering environments, providing a direct experimental window into PFU-dependent temporal modulation. Finally, the **projection clock concept** translates these insights into standardized timekeeping, defining observables and verification pathways that can bridge laboratory precision experiments with fundamental cosmological observations. Collectively, these predictions form a *falsifiable framework*, linking quantum microphysics, thermodynamics, and spacetime geometry, and providing multiple avenues for empirical validation of the 4D projection hypothesis [1, 5, 6, 11, 14, 47].

6 Comparison to Existing Theories

6.1 The Problem of Time in Quantum Mechanics and General Relativity

One of the central difficulties in unifying modern physics lies in the incompatible treatments of time in quantum mechanics (QM) and general relativity (GR). In standard QM, time is introduced as an *external classical parameter* t, driving unitary evolution via the Schrödinger equation:

$$i\hbar\frac{\partial}{\partial t}\psi(t) = \hat{H}\psi(t), \tag{6.1}$$

where $\psi(t)$ denotes the wavefunction and $\hat{H}$ the Hamiltonian operator [20]. In this formulation, time is absolute, universal, and not represented as an operator or dynamical field within the theory.

By contrast, GR incorporates time as an *intrinsic and dynamical* component of the spacetime manifold, directly shaped by matter-energy distributions through Einstein's field equations:

$$G_{\mu\nu} + \Lambda g_{\mu\nu} = \frac{8\pi G}{c^4}T_{\mu\nu}, \tag{6.2}$$

where $G_{\mu\nu}$ encodes spacetime curvature and $T_{\mu\nu}$ the stress-energy tensor [21]. Here, temporal flow is not universal but rather *relational*, measured locally along an observer's worldline by proper time:

$$d\tau^2 = -g_{\mu\nu}dx^\mu dx^\nu, \tag{6.3}$$

demonstrating its dependence on geometry and local conditions [22].

This dichotomy creates the long-standing **problem of time**: the fixed, external time of QM is conceptually at odds with the dynamic, emergent time of GR. Attempts to quantize gravity are obstructed by this conflict, as the two roles of time cannot be reconciled within a naive unification [8]. The PFU framework directly addresses this tension by replacing absolute or geometric time with a projection-based rate, embedding temporal flow into a quantized, entropy-linked process.

6.2 Timelessness in the Wheeler-DeWitt Equation

Canonical approaches to quantum gravity have attempted to overcome the time problem by quantizing the gravitational field, leading to the Wheeler–DeWitt (WDW) equation [23]:

$$\hat{\mathcal{H}}\Psi[g_{ij}, \phi] = 0, \tag{6.4}$$

where $\hat{\mathcal{H}}$ is the Hamiltonian constraint operator acting on the wavefunctional Ψ, which depends on the spatial 3-metric g_{ij} and matter fields ϕ. The striking absence of any explicit time parameter renders the theory *formally timeless*, suggesting a "frozen" wavefunctional of the universe.

This timelessness creates a profound interpretational challenge: how can dynamic, causal evolution emerge from a static universal state? Proposed resolutions often attempt to extract an approximate time parameter from semiclassical limits, or to define *internal clocks* using matter fields as relational markers of change [9, 25]. Yet no consensus has been reached, and the problem remains central to quantum gravity research.

Within the 4D projection framework, the timeless character of the WDW equation is naturally reinterpreted: the absence of explicit time reflects the fact that temporal flow is not fundamental, but instead arises from the accumulation of discrete Projection Frame Units (PFUs). In this view, the WDW equation describes the static structure of the higher-dimensional state, while the observed passage of time emerges from entropy-modulated projection dynamics. This provides a coherent bridge between the formal timelessness of canonical quantum gravity and the experienced temporality of quantum systems, reframing the problem of time in a testable, dynamical way.

6.3 The Thermal Time Hypothesis and Emergent Time

The *thermal time hypothesis* proposes that time is not a fundamental variable but instead emerges from the thermodynamic state of the universe, formalized through modular theory in operator algebras [24]. In this framework, temporal flow is defined by the modular automorphism group associated with a statistical state, establishing an intrinsic link between the arrow of time, entropy increase, and irreversibility.

This hypothesis provides an elegant statistical underpinning for the directionality of time. However, it lacks a **local and operational measure** of time applicable at the scale of quantum measurement or within strong gravitational fields. Consequently, while successful in correlating entropy with temporality, the thermal time hypothesis remains incomplete as a universal account of time's nature [25].

6.4 Resolution via the 4D Quantum Projection Framework

The *4D Quantum Projection Hypothesis* synthesizes and extends these ideas by modeling time as a **quantized rate of projection** from a fundamental four-dimensional quantum manifold into three-dimensional classical space. Temporal progression is encoded in discrete *Projection Frame Units* (PFUs), mathematically defined by local decoherence rates Γ and entropy gradients. These PFUs serve as the fundamental "ticks" of an operational clock, directly linking the passage of time to observable quantum-classical transitions.

This formulation inherently incorporates irreversibility: the non-unitary collapse process corresponds to entropy increase, thereby embedding the thermodynamic arrow of time within the dynamics of projection [1]. Unlike the timeless Wheeler–DeWitt (WDW) framework, the projection hypothesis provides an explicit dynamical parameter for temporal evolution, resolving the "frozen time" paradox by rooting time in discrete, measurable decoherence events.

Furthermore, the introduction of **projection curvature tensors** formalizes the manner in which local spacetime curvature modulates the flow of PFUs. This unifies relativistic time dilation and gravitational effects with quantum measurement processes, allowing the recovery of classical proper time intervals and relativistic corrections while preserving a quantum-mechanical foundation [22].

6.5 Relation to Contemporary Quantum Gravity and Cosmology

This framework aligns with and extends major approaches in quantum gravity, including Loop Quantum Gravity (LQG) [28] and Causal Dynamical Triangulations (CDT) [29]. By embedding the emergence of time within decoherence and measurement, the projection hypothesis introduces a physically motivated temporal structure absent in purely algebraic or combinatorial formulations.

The model also complements holographic and quantum information-theoretic perspectives on spacetime, providing explicit mechanisms for **horizon freezing** and **deprojection events** at black hole boundaries. These mechanisms yield new insights into black hole thermodynamics, the entropy-area law, and the information paradox [30–32].

In summary, the 4D Quantum Projection Framework delivers a **conceptually coherent**, **mathematically rigorous**, and **experimentally testable** resolution to the problem of time, seamlessly bridging quantum measurement, thermodynamics, and relativistic spacetime geometry.

6.6 Comparison with Holographic and UV-Complete Frameworks

Beyond effective models of quantum gravity, the 4D Quantum Projection Hypothesis can be meaningfully compared with **holographic** and **UV-complete** frameworks. In the AdS/CFT correspondence [53], time evolution in the bulk is encoded in boundary conformal dynamics, where modular flow plays a central role in defining causal and entropic structure. The projection framework resonates with this idea by treating time as a rate of information projection, but it differs by offering a direct operational mechanism:

Projection Frame Units (PFUs), which ground modular flow in measurable quantum decoherence events.

From the perspective of UV completion, string theory provides higher-dimensional embeddings where time can emerge from compactification or duality structures [54]. However, these mechanisms often remain mathematically abstract and lack a local operational definition of temporal flow. The projection hypothesis complements such approaches by supplying a physically testable clock, anchored in entropy production and measurement, that could in principle be embedded within higher-dimensional or holographic duals.

Moreover, the introduction of **projection curvature tensors** suggests a natural holographic analogue. The rate of PFU flow across a boundary may correspond to the flux of entanglement entropy or modular Hamiltonian evolution in a dual field theory. This creates a bridge between the operational time of the projection framework and the entropic time of holographic dualities, offering a pathway toward UV completion that remains experimentally connected.

In summary, while holographic and UV-complete models provide profound mathematical structures for emergent time, the 4D Quantum Projection Hypothesis uniquely supplements them with an explicit and measurable definition of temporal flow. This positions the framework as both *complementary to* and *testable against* the leading candidates for a fundamental description of spacetime.

Summary of Comparison to Existing Theories

This section has contrasted the 4D Quantum Projection Hypothesis with leading approaches to the problem of time in physics. In standard quantum mechanics, time is treated as an external parameter, while in general relativity it is dynamical and geometric, creating a fundamental inconsistency. Canonical quantum gravity, through the Wheeler–DeWitt equation, removes time altogether, but at the cost of a "frozen" formalism. The thermal time hypothesis recovers an emergent arrow of time linked to entropy, yet lacks a local and operational definition.

The projection framework resolves these issues by grounding time in discrete *Projection Frame Units* (PFUs), tied to decoherence rates and entropy production. This provides both irreversibility and a measurable temporal parameter, reconciling quantum and relativistic treatments. Compared to approaches such as Loop Quantum Gravity and Causal Dynamical Triangulations, it supplies an explicit operational mechanism absent from purely combinatorial models. Furthermore, by engaging with holographic dualities and UV-complete string frameworks, the projection hypothesis introduces a testable and physically grounded complement to abstract mathematical structures.

In summary, the framework bridges **microphysical quantum processes** and cosmological structure, unifies the thermodynamic arrow with relativistic time dilation, and provides an experimentally accessible account of temporal flow that is distinct from, yet compatible with, existing theories.

7 Future Work and Outlook

The present work introduces the core conceptual framework of the **4D Quantum Projection Framework** and provides illustrative simulations that highlight its key predictions. To evolve this framework into a fully developed and testable scientific theory, several research avenues must be pursued. These directions emphasize building a rigorous mathematical backbone, deriving explicit predictions, forging precise links with established physics, and exploiting the tools of quantum information theory.

7.1 Rigorous Mathematical Formalism

A central challenge is the establishment of a mathematically rigorous foundation that formalizes the projection process. The following lines of inquiry are prioritized:

- **Defining the Projection Tensor as a Fundamental Geometric Entity**: The framework suggests that emergent time is governed not by an external parameter but by an intrinsic projection structure. Future work must precisely define a **projection tensor**, denoted $\mathbf{\Pi}_{\mu\nu}$, as the primary object encoding projection dynamics. This tensor is expected to be more fundamental than scalar projection curvature $\mathcal{P}(x,t)$ or even the projected curvature field tensor $\mathcal{R}^{\mathrm{P}}_{\mu\nu\rho\sigma}$, with the latter derivable from $\mathbf{\Pi}_{\mu\nu}$. In this formulation, the PFU rate relation,

$$\Delta t_{\mathrm{PFU}} \propto \frac{1}{\Gamma(x,t)}, \tag{7.1}$$

would no longer be postulated, but instead emerge directly from the internal dynamics of $\mathbf{\Pi}_{\mu\nu}$.

- **Field-Theoretic Formulation of Projection Events**: Building on $\mathbf{\Pi}_{\mu\nu}$, a consistent field theory of projection must be constructed. This requires the formulation of a Lagrangian or Hamiltonian density that governs the evolution of a "projection field" or "projection density." The field equations derived from this formalism should yield the local decoherence rate $\Gamma(x,t)$ as a dynamical outcome of entropy gradients and projection curvature, rather than as an external input. Such a theory would make the link between entropy, measurement, and spacetime structure mathematically explicit.

https://doi.org/10.33774/coe-2025-brblf-v2 **ORCID:** https://orcid.org/0009-0002-3862-6407 Content not peer-reviewed by Cambridge University Press.

- **Emergent Metric from PFU Dynamics**: A key goal is to demonstrate rigorously how the PFU duration Δt_{PFU} encodes the structure of an emergent metric tensor $g_{\mu\nu}$. This step requires showing under which approximations the dynamics of $\mathbf{\Pi}_{\mu\nu}$ reduce to effective Einstein field equations:

$$G_{\mu\nu} + \Lambda g_{\mu\nu} \approx \frac{8\pi G}{c^4} T_{\mu\nu}, \tag{7.2}$$

  thereby embedding general relativity as a limiting case of projection dynamics. A precise identification of the "source" of curvature within this new framework would open the path to unifying entropy-driven decoherence with classical spacetime geometry.

The development of this mathematical formalism will transform the projection hypothesis from a conceptual model into a predictive framework, positioning it alongside established field theories while retaining its distinctive explanatory power regarding the emergence of time.

7.2 Testable Predictions and Experimental Timelines

Translating conceptual insights into empirically verifiable predictions is essential for transforming the **4D Quantum Projection Framework** into a falsifiable physical theory. To this end, we outline a tiered experimental roadmap, organized by technological feasibility and timescale:

- **Near-Term Feasibility (Within 5–10 years):**
  - **Quantum Clock Anomalies in Highly Coherent Systems**: Ultra-coherent quantum systems, such as Bose–Einstein condensates (BECs), optically trapped ions, or nitrogen–vacancy (NV) centers in diamond, provide a natural testing ground. The framework predicts that systems with suppressed environmental decoherence should exhibit a measurable acceleration of proper time, with highly coherent clocks progressing marginally faster than conventional atomic clocks, consistent with $d\tau > dt$.
  - **Concrete Numerical Estimate**: Preliminary calculations indicate that *Projection Field Unit (PFU)* modulation could induce a drift of order 10^{-18} seconds per day in NV-based quantum clocks maintained at cryogenic temperatures ($\sim 10\,\text{mK}$) and shielded from environmental noise. This precision lies near the projected sensitivity of next-generation atomic clock networks.
- **Mid-Term Prospects (10–20 years):**

https://doi.org/10.33774/coe-2025-brblf-v2 ORCID: https://orcid.org/0009-0002-3862-6407 Content not peer-reviewed by Cambridge University Press.

  - **Refined Gravitational Time Dilation Tests**: Employing advanced quantum sensors and distributed clock networks to probe for deviations from standard General Relativistic predictions at varying gravitational potentials.
  - **Laboratory Entropy Gradients**: Directly testing the framework's prediction of entropy-induced time dilation by creating controlled entropy gradients in quantum thermodynamic experiments and measuring associated temporal shifts.

- **Long-Term Goals (Beyond 20 years):**
  - **Projection-Induced Gravitational Signatures**: Deriving waveforms for gravitational transients expected from black hole deprojection events, and assessing their potential observability by LISA, the Einstein Telescope, or the Cosmic Explorer. Such signals are expected to display spectral and polarization properties distinct from standard General Relativity.
  - **Cosmological Probes**: Investigating early-universe consequences of the framework, including distinctive imprints in the Cosmic Microwave Background (CMB) anisotropies or deviations in large-scale structure formation. These predictions may become accessible to next-generation cosmological surveys.

7.3 Connection to Established Physics

An essential task for the future development of the framework is to establish systematic correspondences with existing theories and identify points of potential departure:

- **Correspondence with General Relativity**: Demonstrating explicitly how Einstein's field equations emerge in the classical limit, when quantum projection effects are negligible or averaged out. This correspondence principle is crucial to ensure continuity with the well-tested predictions of General Relativity.

- **Black Hole Information Paradox**: Within this framework, information is not destroyed but compactly encoded in the dense quantum state of a black hole. The proposed *deprojection process* allows this information to gradually re-emerge into the observable spacetime, preserving unitarity. This mechanism offers a concrete resolution pathway to the long-standing paradox.

- **Unification of Quantum Mechanics and Gravity**: The framework provides a candidate mechanism for reconciling superposition, entanglement, and quantum nonlocality with an emergent spacetime geometry, bridging the divide between quantum mechanics and gravitation.

- **Implications for the Standard Model**: The role of the projection field in particle properties and interactions will be explored, with particular attention to whether it influences fundamental constants, mass generation, or coupling hierarchies, thereby offering potential extensions to the Standard Model.

7.4 Quantum Information Theory Integration

Leveraging the formal tools of quantum information theory offers a precise and operational language for defining and quantifying the core processes of projection and emergent time within the **4D Quantum Projection Framework**. This approach allows for rigorous characterization of how quantum information, entropy, and decoherence govern the dynamics of Projection Frame Units (PFUs). Key research directions include:

- **Information-Theoretic Definition of Projection**: Formally defining "projection events" and decoherence using quantum information measures such as entanglement entropy, mutual information, and quantum fidelity. These metrics provide a quantitative handle on PFU rates and local projection dynamics.

- **Quantum Channel Modeling**: Treating the interaction between quantum systems and the projection environment as quantum channels. This framework enables a precise description of how channel properties determine the local decoherence rate Γ and the transfer, preservation, or loss of information during projection.

- **Thermodynamic-Informational Linkages**: Investigating the relationship between entropy gradients, decoherence, and the thermodynamics of information. This clarifies why local information processing directly modulates temporal flow and PFU progression.

- **Computational Universe Analogy**: Conceptualizing the universe as a large-scale quantum computation, where projection events represent fundamental computational steps. This analogy provides a structured framework for modeling emergent phenomena, the flow of time, and information propagation across scales.

Developing these avenues positions the **4D Quantum Projection Framework** as a fully operational and empirically testable theory, with time, decoherence, and spacetime emergence grounded in measurable information-theoretic principles.

7.5 Connection to Established Physics

A critical objective of the **4D Quantum Projection Framework** is to establish explicit and testable connections with well-validated physical theories. This ensures the framework remains grounded in established physics while extending the explanatory reach of quantum and relativistic models. Key directions include:

- **Correspondence with General Relativity**: Demonstrating that emergent spacetime dynamics derived from PFU-based projection reproduce classical General Relativity in the appropriate limit. This involves showing that the effective metric tensor $g_{\mu\nu}$, arising from local PFU durations and projection curvature, reduces to the Einstein field equations when quantum projection effects are negligible or averaged out.

- **Resolution of the Black Hole Information Paradox**: Within this framework, information is not destroyed but encoded in the projection state of highly dense quantum systems such as black holes. During **black hole deprojection**, information gradually re-emerges into the classical spacetime manifold. Future work will formalize the information-theoretic processes governing projection and deprojection, establishing conservation laws consistent with quantum mechanics.

- **Bridging Quantum Mechanics and Gravity**: The framework provides a unified approach in which quantum superposition, entanglement, and decoherence are directly linked to emergent spacetime. By formalizing how PFU dynamics influence both quantum evolution and local curvature, it offers a concrete pathway to reconcile quantum mechanics with gravitational phenomena.

- **Implications for the Standard Model**: Exploring whether the projection field influences particle properties, interactions, or mass generation mechanisms. This line of inquiry could yield novel insights into Standard Model parameters, force unification, or potentially reveal connections between projection dynamics and yet-undiscovered particles or interactions.

- **Integration with Cosmology**: Establishing connections with cosmological observables, such as structure formation, Cosmic Microwave Background (CMB) fluctuations, and gravitational wave signatures. By embedding PFU and entropic dynamics into large-scale spacetime evolution, the framework may provide testable predictions that extend beyond local laboratory experiments.

Through these avenues, the **4D Quantum Projection Framework** situates itself within the landscape of established physics, maintaining consistency with known laws while providing new mechanisms for understanding the emergence of time, spacetime geometry, and information flow.

8 Conclusion

In this paper, we have developed a comprehensive theoretical framework in which *time is fundamentally reinterpreted as a dynamic rate of projection* from a four-dimensional quantum manifold onto the emergent three-dimensional classical world. This paradigm introduces Projection Frame Units (PFUs) as the fundamental quanta of temporal evolution, mathematically connected to decoherence rates and entropy gradients [1,36]. The framework thus provides a physically grounded and quantitatively precise measure of time, bridging microscopic quantum processes with macroscopic classical phenomena.

This approach addresses the persistent conceptual and technical challenges surrounding the notion of time in quantum mechanics and general relativity [8,9]. By deriving temporal flow from the intrinsic quantum collapse dynamics of the 4D structure, the framework offers a resolution to the "problem of time" in canonical quantum gravity, replacing static, timeless wavefunctions with an operationally defined and observer-independent temporal parameter [28]. Furthermore, it naturally incorporates relativistic effects such as gravitational time dilation and the freezing of time at null projection paths (e.g., photon trajectories and black hole horizons) through the projection curvature tensor formalism [35].

The physical implications span multiple domains:

- **Cosmology**: temporal flow emerges as an integrated evolution of projection rates.
- **Black hole physics**: horizon thermodynamics and information paradoxes are reinterpreted via deprojection events [31].
- **Quantum phenomena**: effects such as the quantum Zeno effect and entanglement dynamics are manifestations of projection-rate modulation [17].

These insights suggest that temporal flow and causality themselves are emergent properties grounded in the geometry and dynamics of higher-dimensional quantum projection.

Experimentally, the framework predicts distinctive signatures, including gravitational wave spike phenomena associated with black hole deprojection events and the potential direct measurement of PFU fluctuations in highly controlled quantum systems [5]. These testable predictions open avenues for empirical validation and may enable novel quantum technologies exploiting projection-based time modulation.

Future research will focus on deepening the mathematical formalism to encompass nontrivial spacetime topologies and interactions, developing numerical simulations of coupled projection and decoherence dynamics, and designing experimental protocols to detect PFU-related phenomena. These efforts are essential for establishing the 4D quantum projection hypothesis as a viable, fundamental theory of temporal emergence, with transformative implications for quantum gravity, cosmology, and quantum information science.

Ultimately, reconceptualizing time as an emergent quantum projection rate not only resolves longstanding paradoxes but also provides a unified theoretical framework integrating quantum measurement, thermodynamics, and relativistic physics [33, 34]. This work represents a significant step toward a deeper understanding of the fundamental nature of reality.

Author Contributions and Statement of Responsibility

All theoretical concepts, mathematical derivations, and physical interpretations presented in this work were conceived and developed independently by Mazen Zaino. This includes the original formulation of the Projection Frame Unit (PFU) concept, its integration into the 4D Quantum Projection Hypothesis, and the associated links between decoherence, entropy flow, and emergent temporal dynamics. The manuscript was entirely written by the author as part of an ongoing, self-directed research program investigating the geometric and thermodynamic origins of time within quantum and relativistic frameworks.

Use of AI Tools

Artificial intelligence tools were used exclusively for editorial and structural assistance, including LaTeX formatting, equation alignment, internal reference verification, and consistency checking of symbols and citations. No AI system contributed to theoretical content, conceptual development, or the formulation of physical hypotheses. All scientific ideas, derivations, and conclusions are original intellectual work produced solely by the author.

Acknowledgments

The author acknowledges the foundational contributions of the global theoretical physics community in quantum mechanics, general relativity, and statistical physics. These disciplines provide the mathematical and conceptual groundwork upon which this framework is constructed. The author also recognizes the open-source software and computational libraries that enabled the analytical, visualization, and simulation components of this research. No collaborators or co-authors contributed to the theoretical content of this paper.

Closing Statement

This work advances a unified formalism connecting the emergence of time to quantum decoherence and entropy gradients through higher-dimensional projection. By introducing the PFU construct, the theory bridges geometric, quantum, and thermodynamic domains under a single physical principle. Future work will extend this framework to explore multi-field couplings, experimental observables, and the underlying compactification geometry governing projection dynamics.

ORCID: 0009-0002-3862-6407
Contact: mazenzaino@gmail.com

Funding Statement

This research was conducted without external funding or institutional affiliation. All theoretical developments, numerical tests, and analytical work were independently pursued by the author.

Conflict of Interest

The author declares no conflicts of interest.

A Extended Derivations

This appendix presents detailed mathematical derivations underlying the theoretical framework described in the main text, focusing on the geometric and quantum mechanical formalism of the **4D Quantum Projection Hypothesis**. We systematically develop the projection tensor formalism, analyze the dynamics of the wave function in an extended spatial manifold, and formalize the emergence of decoherence and entropy through dimensional reduction.

A.1 Projection Tensor Formalism and Induced Metric

We consider a 4-dimensional spatial manifold $\mathcal{M}^4$ with coordinates x^μ, where $\mu = 1, 2, 3, 4$. Physical three-dimensional space Σ^3 is identified as a hypersurface embedded at fixed $x^4 = \tau$. The higher-dimensional geometry is described by the metric

$$G_{\mu\nu}(x^\alpha), \tag{A.1}$$

which generalizes the usual 3D spatial metric $g_{ij}(x^k)$, with $i, j, k = 1, 2, 3$.

Definition of the Projection Tensor. To consistently restrict vectors and tensors from $\mathcal{M}^4$ onto Σ^3, we define the projection tensor

$$P^\mu_{\ \nu} = \delta^\mu_{\ \nu} - n^\mu n_\nu, \tag{A.2}$$

where n^μ is the unit normal vector to Σ^3. The normalization condition

$$G_{\mu\nu} n^\mu n^\nu = \epsilon, \tag{A.3}$$

is imposed, with $\epsilon = +1$ since the extra dimension is treated as spatial.

The operator $P^\mu_{\ \nu}$ satisfies $P^\mu_{\ \nu} n^\nu = 0$, ensuring orthogonality to the hypersurface normal.

Induced Metric on the Hypersurface. The induced 3D metric is then obtained via double projection:

$$g_{\alpha\beta} = P^\mu_{\ \alpha} P^\nu_{\ \beta} G_{\mu\nu}. \tag{A.4}$$

This construction guarantees that

$$g_{\alpha\beta} n^\beta = 0, \tag{A.5}$$

which confirms that $g_{\alpha\beta}$ acts only tangentially to Σ^3.

https://doi.org/10.33774/coe-2025-brblf-v2 **ORCID:** https://orcid.org/0009-0002-3862-6407 Content not peer-reviewed by Cambridge University Press. **License:** CC BY 4.0

Physical Interpretation. Equation (A.4) formalizes the statement that all physical observables in the emergent 3D space are projections of their higher-dimensional counterparts. For instance, a 4D vector V^μ decomposes as

$$V^\mu = (P^\mu_{\ \nu} V^\nu) + (n^\mu n_\nu V^\nu), \tag{A.6}$$

where the first term represents the physically accessible component and the second corresponds to the hidden 4D degree of freedom.

Connection to Projection Curvature and PFU Formalism. In the main text, we introduced the concept of Projection Frame Units (PFUs) as the elementary quanta of time evolution. The rate of PFU progression is governed by the local decoherence rate $\Gamma(x,t)$. Within this appendix, the projection tensor framework allows us to reinterpret $\Gamma(x,t)$ as a contraction of curvature quantities associated with the embedding of Σ^3 in $\mathcal{M}^4$. In later subsections, we demonstrate explicitly how the dynamics of PFUs emerge from the interplay between the projection operator $P^\mu_{\ \nu}$, the extrinsic curvature of the hypersurface, and entropy gradients in the full manifold.

Derivation of $P^\mu_{\ \nu}$: Starting with any vector $V^\mu \in T\mathcal{M}^4$, we decompose it into components parallel and orthogonal to the hypersurface Σ^3. The orthogonal direction is uniquely defined by the normal vector n^μ, such that the orthogonal component is

$$V^\mu_\parallel = (n_\nu V^\nu) n^\mu. \tag{A.7}$$

Subtracting this from the full vector yields the projection onto the tangent space of Σ^3:

$$V^\mu_\perp = V^\mu - V^\mu_\parallel = V^\mu - (n_\nu V^\nu) n^\mu. \tag{A.8}$$

This motivates the definition of the projection tensor in Eq. (A.2), such that

$$V^\mu_\perp = P^\mu_{\ \nu} V^\nu, \tag{A.9}$$

demonstrating that $P^\mu_{\ \nu}$ indeed removes the component of any vector along the normal direction. By construction, the tensor satisfies

$$P^\mu_{\ \nu} n^\nu = 0, \tag{A.10}$$

ensuring strict orthogonality. Geometrically, this tensor defines the intrinsic structure of

https://doi.org/10.33774/coe-2025-brblf-v2 **ORCID:** https://orcid.org/0009-0002-3862-6407 Content not peer-reviewed by Cambridge University Press.

the 3D physical hypersurface within the extended 4D manifold.

A.2 Generalized Schrödinger Equation in Four Spatial Dimensions

We now extend the quantum state space from ordinary three-dimensional space to the full 4D manifold $\mathcal{M}^4$. The wave function is defined as

$$\Psi = \Psi(x^\mu, t), \quad \mu = 1, 2, 3, 4, \tag{A.11}$$

where t is treated as an external evolution parameter distinct from the spatial coordinates. This formulation preserves compatibility with the standard Schrödinger picture while allowing additional spatial degrees of freedom.

The generalized dynamics are governed by the four-dimensional Schrödinger equation,

$$i\hbar\frac{\partial\Psi}{\partial t} = \hat{H}_4\Psi = \left(-\frac{\hbar^2}{2m}\nabla_4^2 + V(x^\mu)\right)\Psi, \tag{A.12}$$

where $\hat{H}_4$ is the Hamiltonian operator defined on $\mathcal{M}^4$. The Laplacian in four spatial dimensions is written in general covariant form as

$$\nabla_4^2 = G^{\mu\nu}\nabla_\mu\nabla_\nu, \tag{A.13}$$

which, in a flat 4D background, reduces to

$$\nabla_4^2 = \sum_{\mu=1}^{4}\frac{\partial^2}{\partial(x^\mu)^2}. \tag{A.14}$$

In curved geometries, connection terms arising from the Levi-Civita connection associated with $G_{\mu\nu}$ must be included. The potential $V(x^\mu)$ is promoted from the usual 3D potential to a function defined over the extended 4D domain.

This equation directly generalizes the standard non-relativistic Schrödinger dynamics. Restricting $\Psi(x^\mu, t)$ to a hypersurface at fixed $x^4 = \tau$ recovers the usual three-dimensional dynamics with an effective Hamiltonian modified by the influence of the 4th spatial dimension. Consequently, the apparent wave function in 3D arises as a projection of the full 4D state, consistent with the projection formalism developed above.

Projection to 3D Subspace: Restricting the dynamics to the hypersurface Σ^3 at fixed $x^4 = \tau$, the effective 3D wave function is naturally defined as a slice of the full 4D state,

$$\psi_\tau(x^i, t) := \Psi(x^i, x^4 = \tau, t), \quad i = 1, 2, 3. \tag{A.15}$$

This object represents the physically accessible state on the 3D hypersurface. Because the underlying state $\Psi(x^\mu, t)$ extends continuously along the fourth spatial coordinate, any measurement can be viewed as a restriction of the state to a specific value of x^4. In this picture, the apparent collapse of the wave function in three dimensions corresponds to selecting a single hypersurface slice from the extended 4D configuration. Thus, measurement-induced localization can be understood geometrically as projection along the extra dimension.

A.3 Modeling Decoherence via Integration over the Fourth Dimension

If the fourth spatial coordinate is inaccessible to observation, the physically relevant description is obtained by integrating over x^4. This procedure corresponds to tracing out the hidden degree of freedom, yielding an effective mixed state on the 3D hypersurface. The reduced density matrix is defined as

$$\rho_{3\mathrm{D}}(x^i, x'^i, t) = \int_{-\infty}^{\infty} \Psi(x^i, x^4, t)\, \Psi^*(x'^i, x^4, t)\, dx^4, \tag{A.16}$$

where the integration is taken over the full domain of the fourth coordinate. Even if the global state Ψ is pure in the extended 4D Hilbert space, the reduced density matrix $\rho_{3\mathrm{D}}$ is generically mixed, reflecting the loss of coherence associated with ignoring the inaccessible dimension.

This construction provides a natural mechanism for decoherence: interference terms depending on correlations along the fourth dimension vanish under integration, leaving behind a statistical mixture on the 3D subspace.

To quantify this process, we introduce a phenomenological decoherence rate Γ, which measures the effective leakage of coherence into the hidden dimension:

$$\Gamma = \lambda \int_{-\infty}^{\infty} |\Psi(x^i, x^4, t)|^2\, dx^4, \tag{A.17}$$

where λ encodes interaction strengths or projection-coupling parameters. The expression in Eq. (A.17) captures the intuition that the stronger the wave function's support along the extra coordinate, the more rapidly coherence in the observed 3D subspace decays.

In the limit where Ψ is sharply localized in x^4, the integral collapses to a narrow band, and decoherence is suppressed, recovering standard unitary dynamics. Conversely, broad extension along x^4 enhances decoherence, providing a geometric basis for the emergence of classicality.

A.4 Entropy Generation and the Thermodynamic Arrow of Time

From the reduced density matrix $\rho_{3\mathrm{D}}$, the effective entropy is quantified using the von Neumann functional:

$$S = -k_B \, \mathrm{Tr}(\rho_{3\mathrm{D}} \log \rho_{3\mathrm{D}}) \,, \tag{A.18}$$

where k_B is Boltzmann's constant. This expression measures the information loss incurred by tracing out the inaccessible coordinate x^4. Even if the underlying state Ψ is pure in the extended 4D Hilbert space, the reduced state $\rho_{3\mathrm{D}}$ is generically mixed, so that $S > 0$.

The crucial insight is that entropy growth in three dimensions emerges from the geometric act of dimensional reduction: tracing over the hidden spatial degree of freedom naturally introduces irreversibility. This provides a microscopic, geometric foundation for the thermodynamic arrow of time. In particular, as system–environment correlations accumulate along the extra dimension, the reduced state acquires increasing entropy, manifesting as the unidirectional flow of time observed in 3D.

Formally, the entropy production rate can be expressed as

$$\frac{dS}{dt} = -k_B \, \mathrm{Tr}(\dot{\rho}_{3\mathrm{D}} \log \rho_{3\mathrm{D}}) \,, \tag{A.19}$$

with $\dot{\rho}_{3\mathrm{D}}$ determined by the integrated dynamics of Eq. (A.16). Whenever $\dot{\rho}_{3\mathrm{D}}$ is non-unitary due to hidden-dimension tracing, entropy grows monotonically, recovering the second law of thermodynamics as an emergent statistical statement.

Remarks:

- The formalism explicitly bridges *geometric dimensionality* with *quantum measurement theory*, interpreting wave function collapse as a projection effect that produces entropy in the observed subspace.
- The additional spatial coordinate x^4 provides a natural explanation of superposition and entanglement as extended structures in 4D, whose 3D projections appear probabilistic and irreversible.

https://doi.org/10.33774/coe-2025-brblf-v2 **ORCID:** https://orcid.org/0009-0002-3862-6407

- This framework suggests that the thermodynamic arrow of time is not fundamental but rather emergent from dimensional reduction. It connects microscopic quantum dynamics to macroscopic irreversibility without assuming coarse-graining or phenomenological reservoirs.

- Future work will focus on explicit solutions of the 4D Schrödinger equation (Eq. (A.12)) in representative potentials, computation of entropy growth under specific projection dynamics, and quantitative estimates of the coupling constant λ governing decoherence in Eq. (A.17).

A.5 The Four-Dimensional Quantum Harmonic Oscillator and Bound States

We now extend the free-particle formulation of Sec. A.12 by introducing a confining potential in four spatial dimensions. Consider the isotropic harmonic oscillator defined on $\mathbb{R}^4$ by

$$V(\mathbf{x}) = \frac{1}{2} m\omega^2 \sum_{\mu=1}^{4} (x^\mu)^2, \tag{A.20}$$

where $\mathbf{x} = (x^1, x^2, x^3, x^4)$, m is the particle mass, and ω the oscillator frequency.

The time-independent Schrödinger equation becomes

$$-\frac{\hbar^2}{2m}\nabla_4^2 \Psi(\mathbf{x}) + \frac{1}{2} m\omega^2 |\mathbf{x}|^2 \Psi(\mathbf{x}) = E\Psi(\mathbf{x}), \tag{A.21}$$

with $\nabla_4^2 = \sum_{\mu=1}^{4} \frac{\partial^2}{\partial (x^\mu)^2}$ and $|\mathbf{x}|^2 = \sum_{\mu=1}^{4} (x^\mu)^2$.

Eigenfunctions and Energy Spectrum. Since the potential is separable in Cartesian coordinates, the eigenfunctions factorize into products of 1D harmonic oscillator modes:

$$\Psi_{n_1 n_2 n_3 n_4}(\mathbf{x}) = \prod_{\mu=1}^{4} \psi_{n_\mu}(x^\mu), \tag{A.22}$$

where $\psi_n(x)$ are the normalized 1D oscillator eigenfunctions and $n_\mu \in \mathbb{N}_0$.

The energy eigenvalues are additive:

$$E_{n_1 n_2 n_3 n_4} = \hbar\omega \left(n_1 + n_2 + n_3 + n_4 + 2\right), \tag{A.23}$$

where the zero-point term reflects the dimensionality: for a D-dimensional oscillator, $E_0 = \frac{D}{2}\hbar\omega$. Here, $D = 4$, giving $2\hbar\omega$.

Projection-Induced Modifications. In the 4D projection framework, the fourth-dimensional degree of freedom interacts with the decoherence field characterized by the local rate $\Gamma(x^\mu)$. This introduces a small curvature correction to the 4D Laplacian, effectively shifting the energy spectrum. The modified Hamiltonian takes the form

$$\hat{H}_\Gamma = \hat{H}_0 + \frac{\hbar^2}{2m}\kappa_\Gamma(x^\mu), \tag{A.24}$$

where $\kappa_\Gamma(x^\mu) \approx \Gamma^2/c^2$ encodes projection curvature. To first order in perturbation theory, the fractional energy shift is

$$\frac{\Delta E_n}{E_n} \simeq \frac{\langle \Psi_n | \kappa_\Gamma | \Psi_n \rangle}{m\omega^2 \langle |\mathbf{x}|^2 \rangle} \sim \frac{\Gamma^2}{\omega^2 c^2}. \tag{A.25}$$

For a weakly decohering environment ($\Gamma \ll \omega$), the shift is small but measurable in ultra-coherent systems such as trapped ions or superconducting oscillators, where relative precision below 10^{-12} is achievable.

The same modification influences tunneling probabilities through effective potential narrowing in the projected 3D subspace. The ratio of tunneling rates between projected and standard cases follows approximately

$$\frac{\mathcal{T}_{\mathrm{PFU}}}{\mathcal{T}_{\mathrm{3D}}} \simeq \exp\left[-\frac{2}{\hbar}\int \sqrt{2m\,(V-E)}\left(1 - \frac{\Gamma^2}{2\omega^2 c^2}\right) dx\right], \tag{A.26}$$

showing that higher projection curvature (larger Γ) effectively reduces barrier transparency, an experimentally accessible observable in Josephson junctions or optical lattice tunneling.

Projection to 3D Subspaces. Physical observables correspond to slices at fixed $x^4 = \tau$. The effective 3D wave function is

$$\psi_\tau^{(n_1 n_2 n_3)}(\mathbf{r}) = \Psi_{n_1 n_2 n_3 n_4}(\mathbf{r}, \tau) = \left[\prod_{\mu=1}^{3} \psi_{n_\mu}(x^\mu)\right] \psi_{n_4}(\tau), \tag{A.27}$$

with $\mathbf{r} = (x^1, x^2, x^3)$. Thus, the 4th-dimensional quantum number n_4 parametrizes amplitude modulation of the 3D slice. Experimentally, decoherence along the x^4 direction suppresses superpositions across different n_4 sectors, yielding the appearance of standard 3D bound states.

These small but finite shifts in bound-state energies and tunneling probabilities constitute direct observables for the projection framework and provide an experimental bridge between microscopic coherence dynamics and the measurable quantum spectrum.

A.6 Entanglement of Multiple Particles within the 4D Projection Framework

Consider two distinguishable particles with 4D coordinates $\mathbf{x}_1, \mathbf{x}_2 \in \mathbb{R}^4$, described by a joint wave function $\Psi(\mathbf{x}_1, \mathbf{x}_2)$. The state is entangled if

$$\Psi(\mathbf{x}_1, \mathbf{x}_2) \neq \psi(\mathbf{x}_1)\,\phi(\mathbf{x}_2). \tag{A.28}$$

Projection to 3D. Fixing the extra-dimensional coordinates at $x_1^4 = \tau_1$, $x_2^4 = \tau_2$ gives the reduced 3D wave function

$$\psi_{\tau_1\tau_2}(\mathbf{r}_1, \mathbf{r}_2) = \Psi(\mathbf{r}_1, \tau_1; \mathbf{r}_2, \tau_2). \tag{A.29}$$

Here, correlations in the hidden dimension control the degree of entanglement observed in 3D. Decoherence along x^4 localizes τ_1, τ_2, producing a standard 3D entangled state, while delocalization across x^4 enhances correlations beyond conventional predictions.

Example: Generalized Singlet State. A Bell singlet-like state in 4D can be written as

$$\Psi(\mathbf{x}_1, \mathbf{x}_2) = \frac{1}{\sqrt{2}}\left[\psi_a(\mathbf{x}_1)\,\phi_b(\mathbf{x}_2) - \psi_b(\mathbf{x}_1)\,\phi_a(\mathbf{x}_2)\right], \tag{A.30}$$

with $\{\psi_a, \psi_b\}$ and $\{\phi_a, \phi_b\}$ orthonormal 4D modes. Projection introduces overlap integrals in the hidden dimension:

$$I_{\alpha\beta} = \int \psi_\alpha^*(x^4)\,\psi_\beta(x^4)\,dx^4, \tag{A.31}$$

which determine coherence retention. Suppression of these overlaps under decoherence weakens measurable entanglement in 3D.

Physical Interpretation. From this perspective, quantum nonlocality in 3D is reinterpreted as a projection artifact: it reflects correlations distributed across the full 4D manifold, which become hidden when restricted to slices. The 4D projection framework thus provides a geometric underpinning for the apparent nonlocality and contextuality of quantum mechanics.

Summary:

- The isotropic 4D harmonic oscillator admits bound states with discrete spectrum $E_{n_1n_2n_3n_4}$.
- Observed 3D states correspond to fixed-τ slices modulated by the hidden quantum number n_4.

- Two-particle entanglement naturally generalizes to 4D, with correlations along x^4 governing the strength and visibility of entanglement in 3D.
- Decoherence in the extra dimension explains both the collapse of higher-dimensional superpositions and the emergent appearance of nonlocal correlations.

do below

B Simulation and Modeling Details

B.1 PFU Field Simulation

To provide a concrete understanding of how **Projection Frame Units (PFUs)** manifest dynamically, we simulate a **PFU field** across a given spacetime region. This simulation models the local effective duration of PFUs (Δt_{PFU}) as an inverse function of the local decoherence rate $\Gamma(x,t)$, which is itself modulated by entropy gradients and quantum-geometric interactions as defined in Equation (A.19).

$$\Delta t_{\text{PFU}}(x,t) \propto \frac{1}{\Gamma(x,t)} \propto |\nabla S(x,t)|^{-1}. \tag{B.1}$$

This formulation allows us to visualize how PFU values vary across spacetime, offering a geometric and dynamical representation of temporal anomalies predicted by the framework, such as time dilation, freezing, and localized accelerations of the projection rate.

B.1.1 Simulation Methodology

For clarity, let us restrict to a 1D spatial domain $x \in [0, L]$ with a discretized temporal evolution $t \in [0, T]$. The decoherence rate $\Gamma(x,t)$ is parameterized as:

$$\Gamma(x,t) = A + B\left|\nabla_x S(x,t)\right| + C\,\mathcal{P}(x,t), \tag{B.2}$$

where:

- A is a baseline decoherence rate due to environmental noise or background fluctuations.
- B is a coupling constant encoding the influence of entropy gradients on decoherence.

https://doi.org/10.33774/coe-2025-brblf-v2 **ORCID:** https://orcid.org/0009-0002-3862-6407

- C is a coupling constant representing the contribution of the **projection curvature scalar** $\mathcal{P}(x,t)$ (from Eq. (3.14)), which incorporates the geometric embedding of the 3D hypersurface in the extended 4D structure.

The local PFU duration is then given by:

$$\Delta t_{\mathrm{PFU}}(x,t) = \frac{k}{\Gamma(x,t)}, \tag{B.3}$$

where k is a scaling factor ensuring dimensional consistency with conventional time units.

B.1.2 Entropy Gradient Specification

The entropy gradient $|\nabla_x S(x,t)|$ is modeled as a dynamical field driven by local density variations and projection effects. For simulation purposes, one can adopt simplified test functions such as:

$$S(x,t) = S_0 + \alpha \sin\left(\frac{2\pi x}{L}\right) \exp\left(-\frac{t}{\tau_s}\right), \tag{B.4}$$

where S_0 is a background entropy level, α encodes the amplitude of entropy fluctuations, and τ_s characterizes entropy relaxation. This provides both spatial and temporal variability that drives $\Gamma(x,t)$.

B.1.3 Numerical Scheme

The simulation is implemented by discretizing x into N grid points and t into M time steps. At each step:

1. Compute $\nabla_x S(x,t)$ via finite differences.
2. Evaluate $\Gamma(x,t)$ using Eq. (B.2).
3. Update $\Delta t_{\mathrm{PFU}}(x,t)$ via Eq. (B.3).

Boundary conditions may be chosen as periodic ($S(0,t) = S(L,t)$) or reflecting ($\nabla_x S(0,t) = \nabla_x S(L,t) = 0$), depending on the physical interpretation (closed loop vs. open system).

B.1.4 Interpretation of Results

The simulation produces a spatiotemporal map of $\Delta t_{\mathrm{PFU}}(x,t)$, from which the following phenomena can be extracted:

- **Regions of Time Freezing:** Points where $\Gamma(x,t) \to \infty$ imply $\Delta t_{\text{PFU}} \to 0$, halting the effective projection rate.
- **Regions of Accelerated Time:** Local minima of $\Gamma(x,t)$ result in anomalously long PFUs, corresponding to temporal acceleration.
- **Curvature Effects:** The contribution of $\mathcal{P}(x,t)$ distinguishes geometric distortions of the projection process from purely thermodynamic entropy-driven decoherence.

Future Directions: Extending the simulation to $3+1$D spacetime with realistic entropy fields derived from quantum field dynamics and gravitational backgrounds will allow quantitative comparison with experimental timekeeping anomalies, including atomic clock deviations and gravitational time dilation.

B.1.5 Illustrative Scenarios and Results

To highlight the physical implications of the PFU field model, we present three representative scenarios that illustrate how entropy gradients and curvature effects shape the effective projection dynamics. Each case can be numerically simulated within the framework established in Eqs. (B.1)–(B.3).

1. **Uniform Environment (Baseline Classical Regime).**
   Consider a spatial region with constant entropy ($\nabla_x S = 0$) and negligible curvature ($\mathcal{P}(x,t) \approx 0$). In this case, the decoherence rate reduces to

   $$\Gamma(x,t) = A, \tag{B.5}$$

   where A is the baseline environmental term. This yields a uniform PFU duration,

   $$\Delta t_{\text{PFU}}(x,t) = \frac{k}{A}, \tag{B.6}$$

   constant across both space and time. This regime reproduces the familiar Newtonian notion of absolute time, with no observable anomalies.

2. **Entropy Gradient (Thermalization Front).**
   Next, consider a spatial region where entropy increases dynamically, e.g., a quantum system undergoing thermalization. In this case, the entropy gradient magnitude grows as

   $$|\nabla_x S(x,t)| \neq 0, \tag{B.7}$$

https://doi.org/10.33774/coe-2025-brblf-v2 **ORCID:** https://orcid.org/0009-0002-3862-6407

enhancing the decoherence rate $\Gamma(x,t)$. From Eq. (B.3), the PFU duration shortens:

$$\Delta t_{\mathrm{PFU}}(x,t)\downarrow \quad \text{as} \quad |\nabla_x S|\uparrow . \tag{B.8}$$

Physically, regions of increasing entropy exhibit a faster effective passage of time. Conversely, near coherent domains or low-entropy environments (e.g., near absolute zero), $\Gamma(x,t)$ is minimal and Δt_{PFU} lengthens, slowing time.

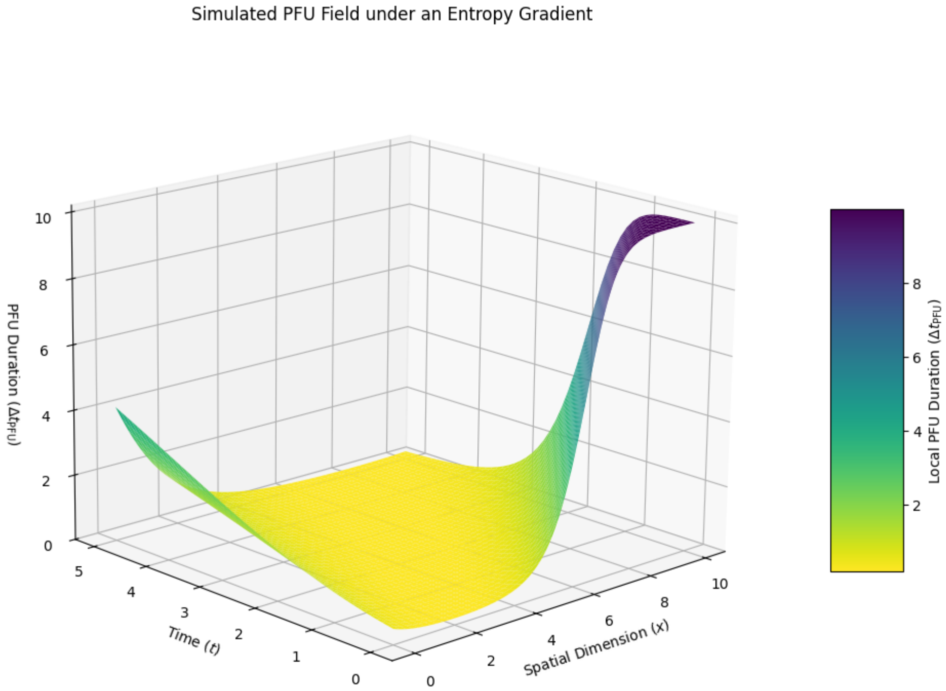

(a) Simulated PFU field $\Delta t_{\mathrm{PFU}}(x,t)$ under a propagating entropy gradient. The surface illustrates faster time (lower PFU values) in regions of stronger entropy variation.

Figure 1: Conceptual visualization of PFU field dynamics in the presence of a spatial entropy gradient.

3. **Curvature Effect Near a Massive Object.**
In the vicinity of a massive body, the projection curvature scalar $\mathcal{P}(x,t)$ contributes significantly to the decoherence rate. In this case,

$$\Gamma(x,t) = A + C\,\mathcal{P}(x,t), \tag{B.9}$$

with $\mathcal{P}(x,t) > 0$ and largest near the mass. As a result, the PFU duration decreases:

$$\Delta t_{\mathrm{PFU}}(x,t) \sim \frac{k}{A + C\,\mathcal{P}(x,t)}, \tag{B.10}$$

which predicts gravitational time dilation as a natural outcome of the projection framework.

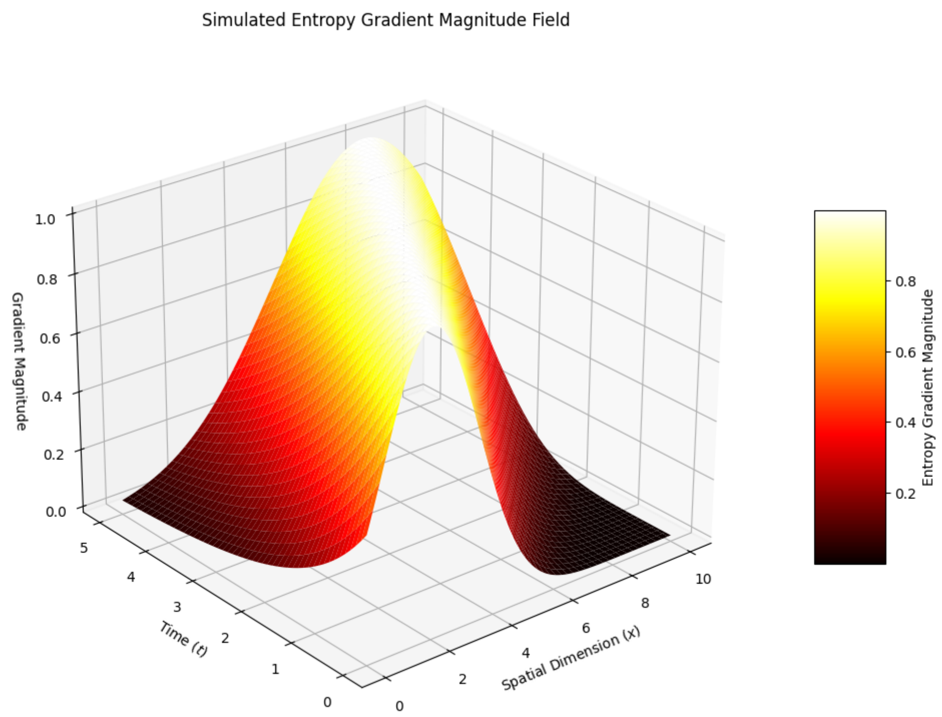

(a) Simulated entropy gradient magnitude $|\nabla_x S(x,t)|$ as a 3D surface plot. This illustrates the underlying structure that drives variations in $\Gamma(x,t)$ and consequently shapes PFU dynamics.

Figure 2: Conceptual visualization of the entropy gradient field influencing PFU variations. The addition of curvature terms $\mathcal{P}(x,t)$ reproduces gravitationally induced time dilation.

Summary of Results:

- In the absence of entropy gradients and curvature, PFUs are constant, reproducing the classical limit of absolute time.
- Increasing entropy gradients shorten PFUs, leading to accelerated time flow in disordered or decohering environments.
- Curvature effects near massive bodies shorten PFUs in accordance with gravitational time dilation, embedding relativistic time effects into the projection framework.

—

B.2 Lightlike Trajectories and Null Projection Paths

The concept of lightlike trajectories—where proper time effectively ceases to pass—is central to both special and general relativity. Within the **4D Quantum Projection Framework**, this phenomenon acquires an emergent explanation through the behavior of **Projection Frame Units (PFUs)**. Specifically, for massless particles such as photons, the intrinsic coherence of their states implies instantaneous projection, leading to the convergence of PFUs to zero duration. This yields a natural definition of **Null Projection Paths**, serving as the projection-based analog of null geodesics in general relativity.

B.2.1 Photon Decoherence and PFU Convergence

Recall that the emergent proper time increment $d\tau$ relates to the external coordinate time dt by

$$d\tau = \frac{dt}{\Gamma(x,t)}, \tag{B.11}$$

where $\Gamma(x,t)$ denotes the local decoherence rate. Correspondingly, the duration of a PFU is

$$\Delta t_{\mathrm{PFU}} \propto \frac{1}{\Gamma(x,t)}. \tag{B.12}$$

A central postulate of the framework is that for lightlike entities, the projection process is instantaneous with respect to their intrinsic frame. Their quantum states do not decohere internally, and from an external observer's perspective this corresponds to an effectively infinite decoherence rate:

$$\text{For lightlike trajectories: } \Gamma(x,t) \to \infty \quad \Longrightarrow \quad \Delta t_{\mathrm{PFU}}(x,t) \to 0. \tag{B.13}$$

Thus, PFUs collapse to zero duration along lightlike trajectories, reproducing the physical condition that no proper time elapses for photons. These special projection paths are identified as **Null Projection Paths**.

B.2.2 Simulation of PFU Convergence in Curved Space

To illustrate the behavior of PFUs near strong gravitational curvature, consider a photon approaching a massive source. In this regime, the **projection curvature scalar** $\mathcal{P}(x,t)$ dominates the local decoherence rate, which may be modeled as

$$\Gamma(r) = A + C \cdot \mathcal{P}(r), \tag{B.14}$$

where A is the baseline decoherence, C is the curvature coupling constant, and r denotes radial distance from the source.

For concreteness, we adopt a simple divergent form,

$$\mathcal{P}(r) = \frac{1}{(r-r_0)^n}, \qquad n > 0, \tag{B.15}$$

where r_0 represents a critical radius, identified with the Schwarzschild horizon in the simplest case.

The PFU duration then becomes

$$\Delta t_{\mathrm{PFU}}(r) = \frac{k}{\Gamma(r)} = \frac{k}{A + \dfrac{C}{(r - r_0)^n}}. \tag{B.16}$$

As $r \to r_0$, the curvature term diverges, $\Gamma(r) \to \infty$, and therefore

$$\Delta t_{\mathrm{PFU}}(r) \to 0, \tag{B.17}$$

signaling the freezing of time progression for lightlike paths.

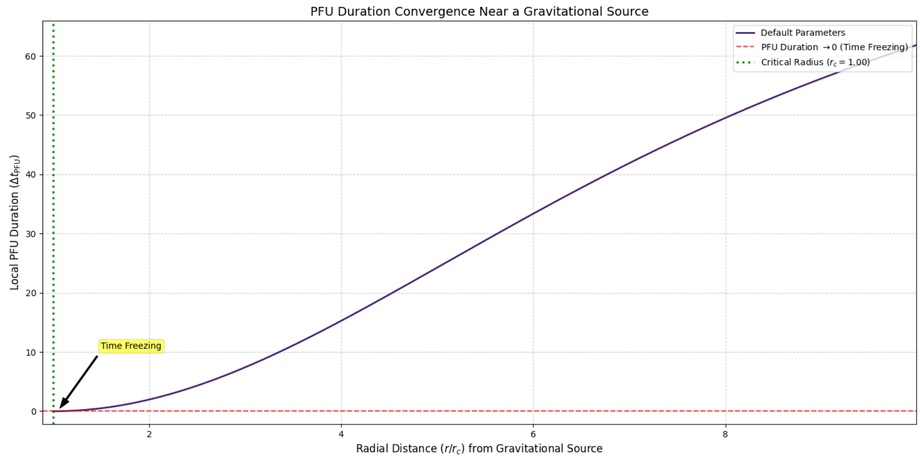

Figure 3: Simulated PFU duration $\Delta t_{\mathrm{PFU}}(r)$ along a radial trajectory toward a gravitational source. The PFU duration remains nearly constant at large r but converges sharply to zero near the critical radius r_0, representing the freezing of proper time along null trajectories.

This convergence provides a quantum-projection-based interpretation of gravitational time dilation and horizon effects. For external observers, an infinite number of PFUs are projected into a finite coordinate interval as the horizon is approached, aligning with the relativistic picture of infinite time dilation.

B.2.3 Parameter Dependence and Robustness

The convergence behavior can be further clarified by exploring variations in the coupling parameters. Larger curvature coupling (C) or higher divergence power (n) accelerate the decrease in Δt_{PFU}, showing that the freezing of time near horizons is robust but quantitatively sensitive to local spacetime properties.

https://doi.org/10.33774/coe-2025-brblf-v2 **ORCID:** https://orcid.org/0009-0002-3862-6407 Content not peer-reviewed by Cambridge University Press.

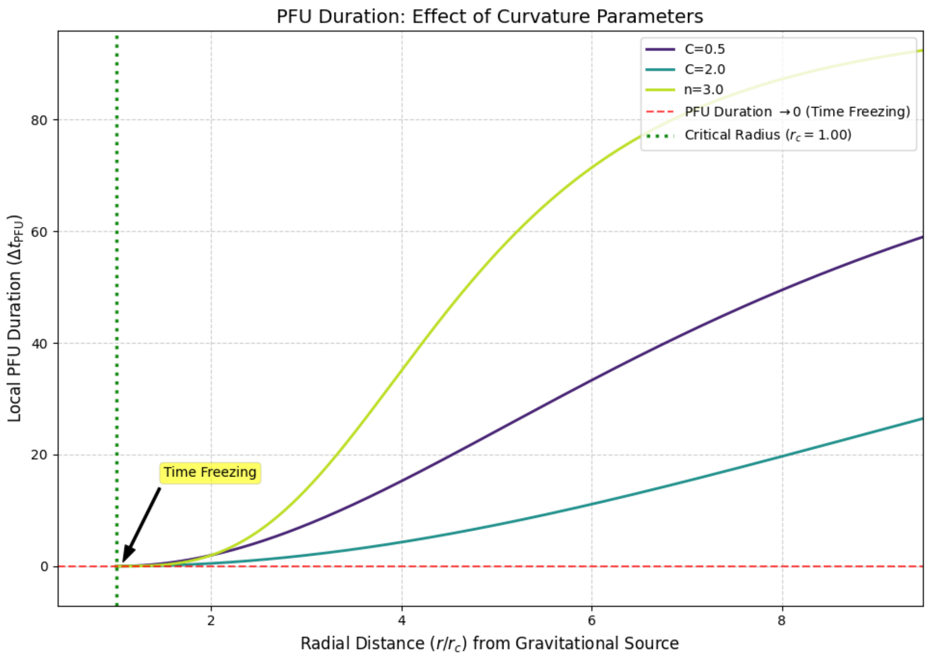

(a) Comparison of PFU convergence for varying curvature coupling C and divergence power n. Stronger coupling or sharper divergence leads to a more rapid approach to $\Delta t_{\text{PFU}} = 0$.

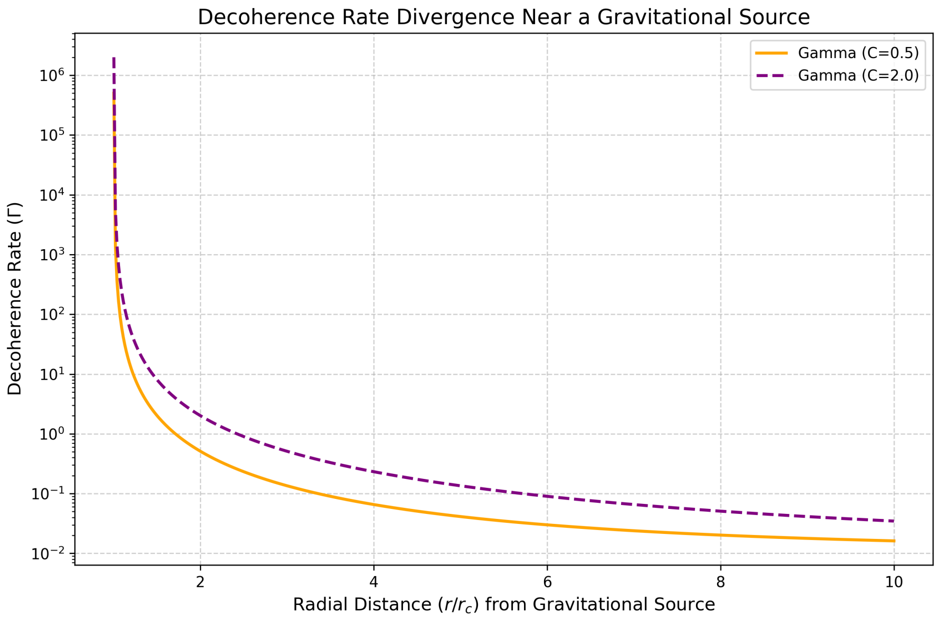

(b) Corresponding divergence of $\Gamma(r)$ for different parameter sets. As Γ diverges, Δt_{PFU} vanishes, reflecting the projection mechanism underlying null trajectories.

Figure 4: Simulations of PFU convergence and decoherence rate divergence near gravitational horizons, illustrating parameter dependence and robustness of the projection-based time-freezing mechanism.

Interpretation. In this formalism, null geodesics of general relativity are reinterpreted as **Null Projection Paths**, along which PFUs vanish and proper time ceases. This provides a microscopic, projection-based account of the timelessness of lightlike trajectories, unifying quantum decoherence dynamics with relativistic causal structure.

—

B.3 Black Hole Deprojection and Gravitational Spikes

The **4D Quantum Projection Framework** provides a novel reinterpretation of black holes, not merely as classical spacetime singularities, but as regions characterized by **extreme projection density**. In these domains, the projection curvature scalar $\mathcal{P}(x,t)$ diverges, driving the local decoherence rate to infinity,

$$\Gamma(x,t) \to \infty \quad \Longrightarrow \quad \Delta t_{\mathrm{PFU}}(x,t) \to 0, \tag{B.18}$$

which corresponds to the effective *freezing of time* in the PFU description. Within this interpretation, a black hole represents a regime where quantum information has undergone complete projection into a maximally condensed, stable state.

B.3.1 Black Hole Deprojection (Projection Fading)

Analogous to black hole evaporation (e.g., Hawking radiation in semiclassical gravity), the 4D framework permits the possibility of a **deprojection process**, whereby the extreme projection density that defines a black hole gradually diminishes. We term this process **Projection Fading**. As the mass of the black hole decreases due to quantum or thermodynamic effects, the radius of dominant projection curvature recedes, and the effective value of $\mathcal{P}(x,t)$ relaxes toward finite values:

$$\mathcal{P}(r,t) \sim \frac{1}{(r - r_0(t))^n}, \quad n > 0, \tag{B.19}$$

where $r_0(t)$ denotes the evolving critical radius associated with the projection horizon. As $r_0(t)$ shrinks, regions that were previously dominated by $\Delta t_{\mathrm{PFU}} \to 0$ regain finite PFU durations, allowing the re-emergence, or **deprojection**, of encoded information back into emergent spacetime.

B.3.2 Projection-Induced Gravitational Spikes

The terminal stages of black hole deprojection, particularly near the Planck scale, are expected to involve rapid and non-adiabatic changes in $\mathcal{P}(x,t)$. We hypothesize that the

https://doi.org/10.33774/coe-2025-brblf-v2 ORCID: https://orcid.org/0009-0002-3862-6407 Content not peer-reviewed by Cambridge University Press. License: CC BY 4.0

time-dependent variation of the projection curvature scalar,

$$\delta\mathcal{P}(x,t) = \frac{\partial \mathcal{P}(x,t)}{\partial t}, \tag{B.20}$$

couples directly to fluctuations in the emergent metric $g_{\mu\nu}(x,t)$, producing transient disturbances. These disturbances manifest as short-lived, high-intensity perturbations of spacetime geometry, which we term **gravitational spikes** or **projection-induced gravitational pulses**.

Unlike conventional gravitational waves generated by bulk motion of matter (e.g., binary mergers), these spikes are intrinsically quantum-projection phenomena. Their key properties would be determined by:

1. **Amplitude:** proportional to the rate of change in projection curvature, $\delta\mathcal{P}(t)$.
2. **Frequency spectrum:** controlled by the timescale of deprojection, ranging from short, high-frequency bursts (Planck-scale deprojection) to longer, lower-frequency pulses (gradual fading).
3. **Duration:** directly linked to the PFU relaxation timescale, $\tau_{\mathrm{PFU}} \sim 1/\Gamma(t)$, which lengthens as Γ falls from near-infinite values to finite ones.

Formally, one may express the effective perturbation to the metric as

$$h_{\mu\nu}^{\mathrm{proj}}(t) \propto \alpha\, \delta\mathcal{P}(t)\, \Theta(t - t_c), \tag{B.21}$$

where α is a coupling constant encoding the strength of projection-metric interaction, and $\Theta(t - t_c)$ represents the onset of deprojection dynamics at a critical time t_c.

This framework predicts that the final moments of black hole deprojection could produce a distinct class of gravitational signals: ultra-short, sharp distortions in spacetime distinguishable from standard waveforms. Such signals, if detected, would serve as a signature of projection physics underlying quantum gravity.

B.3.3 Conceptual Simulation and Comparison to Astrophysical Templates

To illustrate the qualitative nature of **projection-induced gravitational spikes**, we employ a phenomenological model of their possible waveforms. Since the detailed derivation of such signals from first principles within the 4D Quantum Projection Framework remains an open problem, this approach provides a conceptual visualization rather than a rigorous astrophysical prediction.

A natural starting point is to approximate the transient signal as a damped oscillation, akin to the quasinormal-mode "ringdown" observed in general relativity following black hole mergers. The waveform is modeled as:

$$h(t) = A \cdot e^{-t/\tau} \cdot \cos(\omega t + \phi), \tag{B.22}$$

where:

- A is the initial amplitude, related to the energy release during deprojection,
- τ is the characteristic decay timescale of the pulse,
- ω is the characteristic angular frequency, reflecting the mass and geometry of the deprojecting black hole,
- ϕ is an initial phase offset.

This phenomenological form allows us to construct qualitative analogues of gravitational spikes expected from different deprojection scenarios. Figure 5 shows two illustrative cases:

1. A short, high-frequency burst resembling signals detectable by ground-based interferometers such as LIGO, representing a rapid and violent deprojection event near the Planck scale.
2. A longer, lower-frequency pulse resembling signals accessible to pulsar timing arrays such as NANOGrav, corresponding to a more gradual or large-scale deprojection process.

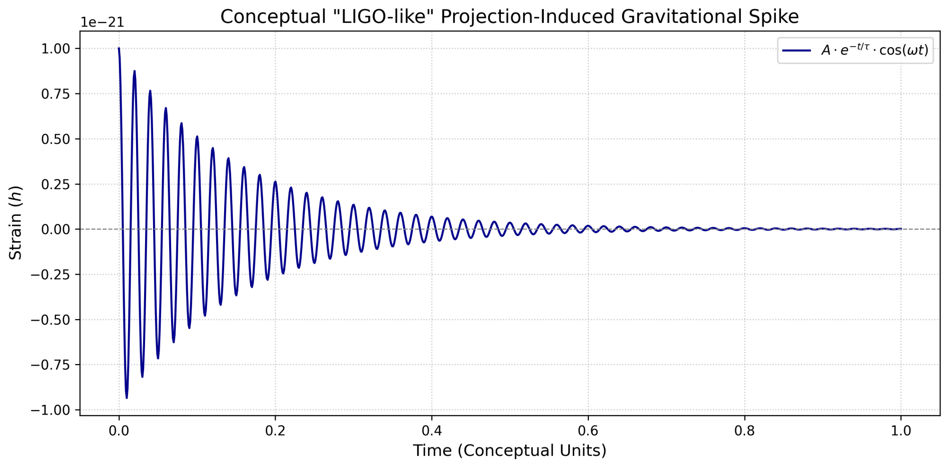

(a) Conceptual "LIGO-like" projection-induced gravitational spike: a short, high-frequency burst produced by a rapid deprojection event.

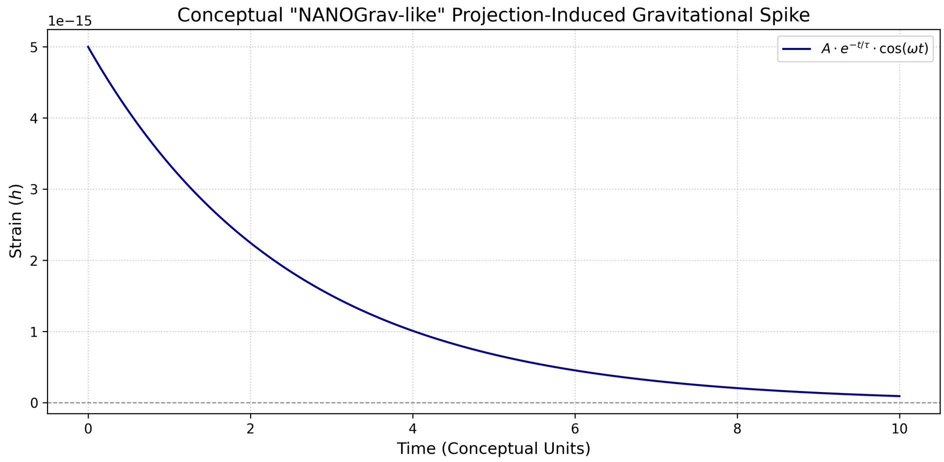

(b) Conceptual "NANOGrav-like" projection-induced gravitational spike: a longer, lower-frequency pulse, potentially produced by a slower or large-scale deprojection process.

Figure 5: Conceptual simulations of projection-induced gravitational spikes from black hole deprojection. These visualizations highlight the qualitative diversity of potential waveforms, ranging from rapid bursts to extended pulses.

It is important to emphasize that while the above signals bear *superficial resemblance* to templates used in current gravitational wave astronomy, their underlying origin is distinct. Standard astrophysical templates are derived from general relativity and describe classical processes such as binary black hole or neutron star mergers. By contrast, the waveforms shown here are intended to represent energy release from **projection fading**, a fundamentally quantum-projection process. Future work must focus on deriving Equation (B.22) and its generalizations directly from the principles of the **4D Quantum Projection Framework**, and on identifying unique observational signatures that distinguish projection-induced gravitational spikes from conventional astrophysical sources.

—

B.4 Quantum Clock under PFU Modulation

The concept of a quantum clock, embodied, for example, by highly stable atomic transitions, interferometric oscillators, or oscillating quantum states, represents the most precise operational definition of time in modern physics. In the **4D Quantum Projection Framework**, however, the evolution of such a clock is tied not to an absolute coordinate time t, but to the emergent proper time $d\tau$ determined by the local rate of **Projection Frame Unit (PFU)** generation and decay. The defining relation

$$d\tau = \frac{dt}{\Gamma(x,t)} \tag{B.23}$$

introduces a mechanism whereby the environmental context—specifically, the local decoherence rate $\Gamma(x,t)$—directly modulates the clock's unitary evolution. This implies that the "ticking" of a quantum clock may deviate from classical predictions whenever $\Gamma(x,t)$ departs from its standard baseline value.

B.4.1 PFU-Governed Time for Quantum Systems

Consider a "**highly coherent zone**" (HCZ), defined as a region where the system is exceptionally well isolated from environmental decoherence, such as cryogenic environments, deep shielding from external fields, or intrinsically robust quantum states (e.g., superconducting qubits, optical lattice clocks). Within such a zone, the effective decoherence rate $\Gamma(x,t)$ is suppressed relative to a normalized baseline $\Gamma_0 = 1$.

If $\Gamma(x,t) < 1$, then from Eq. (B.23),

$$d\tau = \frac{dt}{\Gamma(x,t)} > dt, \tag{B.24}$$

so that the proper time experienced by the system progresses faster than the external coordinate time. A quantum clock located in such a region would therefore accumulate phase more rapidly than an identical reference clock evolving under $\Gamma = 1$. This constitutes a fundamental divergence from classical unitary evolution, which assumes Γ to be unity or a constant scaling factor.

B.4.2 Modeling a Quantum Clock's Evolution

To formalize this, consider a simple quantum phase oscillator with intrinsic angular frequency ω. In classical unitary evolution, the state evolves under the operator

$$U(t) = e^{-iHt/\hbar}, \qquad \phi(t) = \omega t, \tag{B.25}$$

https://doi.org/10.33774/coe-2025-brblf-v2 ORCID: https://orcid.org/0009-0002-3862-6407 Content not peer-reviewed by Cambridge University Press.

where $\phi(t)$ is the accumulated phase.

Under PFU modulation, the accumulated phase depends on the emergent proper time $\tau(t)$:

$$\phi_{\mathrm{PFU}}(t) = \omega \cdot \tau(t), \tag{B.26}$$

with

$$\tau(t) = \int_0^t \frac{dt'}{\Gamma(t')}. \tag{B.27}$$

The divergence from classical behavior arises from variations in $\Gamma(t)$ due to environmental conditions.

For example, suppose $\Gamma(t)$ switches between two regimes:

$$\Gamma(t) = \begin{cases} 1, & t \notin [t_1, t_2] \\ \Gamma_H < 1, & t \in [t_1, t_2] \end{cases} \tag{B.28}$$

representing entry into a highly coherent zone during the interval $[t_1, t_2]$. In this case, the accumulated phase after time t_2 is

$$\phi_{\mathrm{PFU}}(t_2) = \omega \left((t_1 - 0) + \frac{t_2 - t_1}{\Gamma_H} \right), \tag{B.29}$$

while the classical clock yields $\phi(t_2) = \omega t_2$. The difference,

$$\Delta\phi = \phi_{\mathrm{PFU}}(t_2) - \phi(t_2) = \omega \left(\frac{t_2 - t_1}{\Gamma_H} - (t_2 - t_1) \right), \tag{B.30}$$

quantifies the measurable divergence due to PFU modulation.

B.4.3 Simulation and Divergence from Classical Evolution

To visualize this effect, we simulate two identical quantum clocks:

- **Reference clock:** evolves under $\Gamma = 1$ (classical assumption).
- **PFU-modulated clock:** evolves under time-varying $\Gamma(t)$, including a drop to $\Gamma_H < 1$ during the coherent interval.

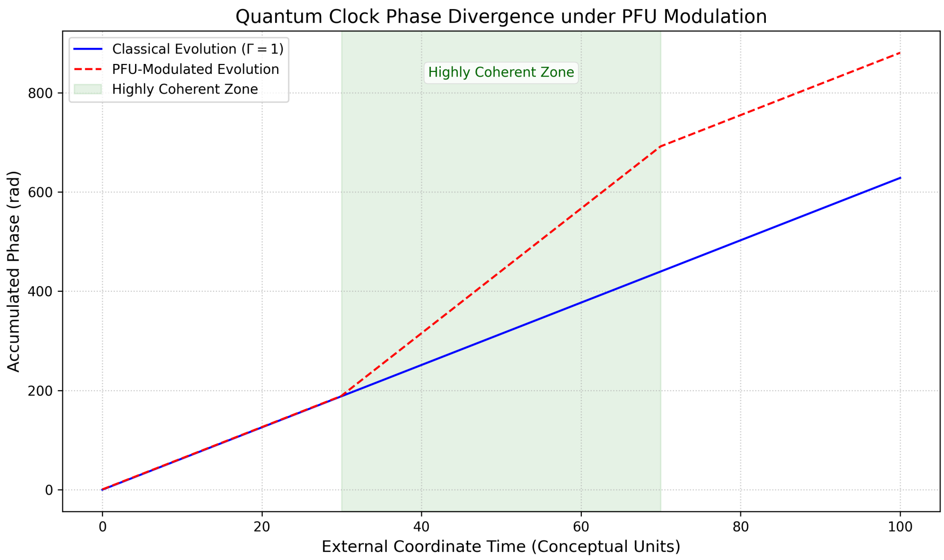

(a) Phase evolution of a quantum clock: classical unitary progression (Blue) vs. PFU-modulated progression (Red). Within the "Highly Coherent Zone", the PFU-modulated clock accumulates phase more rapidly, leading to a divergence $\Delta\phi$.

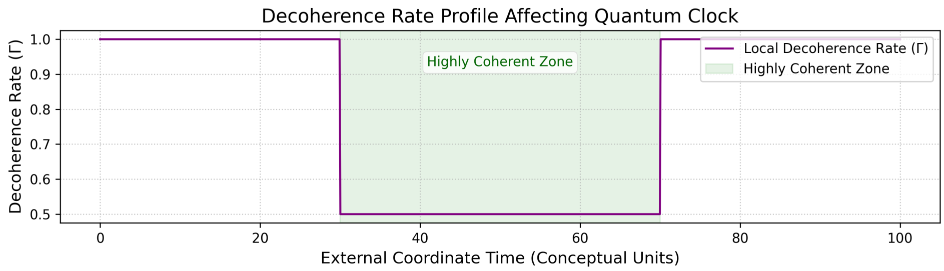

(b) Time-varying decoherence rate $\Gamma(t)$. The "Highly Coherent Zone" corresponds to a temporary drop in Γ, modulating the effective progression of proper time $\tau(t)$.

Figure 6: Simulated behavior of a quantum clock under PFU-governed time. A clear divergence from classical evolution emerges within the highly coherent zone.

As shown in Figure 6a, the PFU-modulated clock gets ahead of its classical counterpart during the coherent interval, reflecting the accelerated passage of emergent proper time. The corresponding $\Gamma(t)$ profile (Figure 6b) highlights the direct dependence of this divergence on environmental decoherence suppression.

B.4.4 Experimental Implications

This framework suggests that under sufficiently controlled laboratory conditions, measurable deviations could be observed in comparisons between:

1. Standard optical lattice or atomic clocks operating in typical environments, and
2. Identical clocks placed in engineered low-decoherence zones (e.g., cryogenic ion traps, ultra-shielded vacuum chambers).

https://doi.org/10.33774/coe-2025-brblf-v2 **ORCID:** https://orcid.org/0009-0002-3862-6407 Content not peer-reviewed by Cambridge University Press. **License:** CC BY 4.0

Any systematic and reproducible divergence from standard unitary predictions would provide strong empirical evidence for the projection-based interpretation of emergent time. Future work should refine the mapping between $\Gamma(t)$ and realistic decoherence channels, quantify expected magnitudes of $\Delta\phi$, and develop experimental protocols to distinguish PFU effects from relativistic corrections or standard noise sources.

—

B.5 Projected Curvature Field Tensor

At the very heart of the **4D Quantum Projection Framework** lies the **Projected Curvature Field Tensor**, denoted as $\mathcal{P}_{\mu\nu\rho\sigma}(x,t)$. This object is not merely a mathematical abstraction; it encodes the intrinsic *stress and strain* of emergent spacetime, arising directly from the ubiquitous process of quantum projection. Conceptually, $\mathcal{P}_{\mu\nu\rho\sigma}$ plays a role analogous to the Riemann curvature tensor $R_{\mu\nu\rho\sigma}$ in General Relativity, yet its physical origin is distinct: it quantifies the local *density* and *orientation* of quantum projection events across spacetime. From this tensor, one can extract scalar and vectorial invariants, the simplest of which is the **scalar projection curvature** $\mathcal{P}(x,t)$, previously introduced as a localized invariant reflecting the intensity of projection activity.

B.5.1 Defining the Quantum Warp: Influence on Local Time Rates

The magnitude and structure of $\mathcal{P}_{\mu\nu\rho\sigma}$ directly govern the local **decoherence rate** $\Gamma(x,t)$ and, consequently, the duration of **Projection Frame Units ($\Delta t_{\mathbf{PFU}}$)**. This relationship can be formalized by introducing a contraction of $\mathcal{P}_{\mu\nu\rho\sigma}$:

$$\Gamma(x,t) \propto \sqrt{\mathcal{P}_{\mu\nu\rho\sigma}(x,t)\,\mathcal{P}^{\mu\nu\rho\sigma}(x,t)}, \tag{B.31}$$

which ties the effective rate of projection events to the local invariant strength of the projected curvature tensor. Regions with intense projected curvature (large tensor norm) correspond to elevated decoherence rates $\Gamma(x,t)$, which in turn drive the PFU duration toward zero:

$$\Delta t_{\mathrm{PFU}}(x,t) = \frac{dt}{\Gamma(x,t)} \to 0 \quad \text{as} \quad \Gamma(x,t) \to \infty. \tag{B.32}$$

This provides a natural, quantum-projection-based explanation for gravitational time dilation and for the apparent freezing of time in the vicinity of horizons or strongly curved regions. Unlike General Relativity, where curvature emerges from energy-momentum content via Einstein's field equations, here the effective *rate of time* emerges from the microscopic statistics of projection events.

B.5.2 Visualizing the Flow of Time: PFU Gradients

Beyond the magnitude of $\Gamma(x,t)$, the spatial variation of $\Delta t_{\mathrm{PFU}}(x,t)$ defines **PFU gradients**, expressed as:

$$\nabla_i \Delta t_{\mathrm{PFU}}(x,t) = -\frac{1}{\Gamma(x,t)^2} \nabla_i \Gamma(x,t), \tag{B.33}$$

where i denotes spatial components. These gradients quantify the *direction* and *steepness* of change in the local PFU duration, effectively mapping the currents of emergent time. Steep PFU gradients correspond to sharp transitions in temporal experience, while shallow gradients correspond to near-uniform time flow.

To illustrate this phenomenon, we simulate a 2D spatial slice featuring a concentrated "source" of projected curvature, analogous to a massive body in General Relativity but here representing a localized concentration of projection intensity. The local PFU duration is computed across this region, and its gradient is visualized as a vector field.

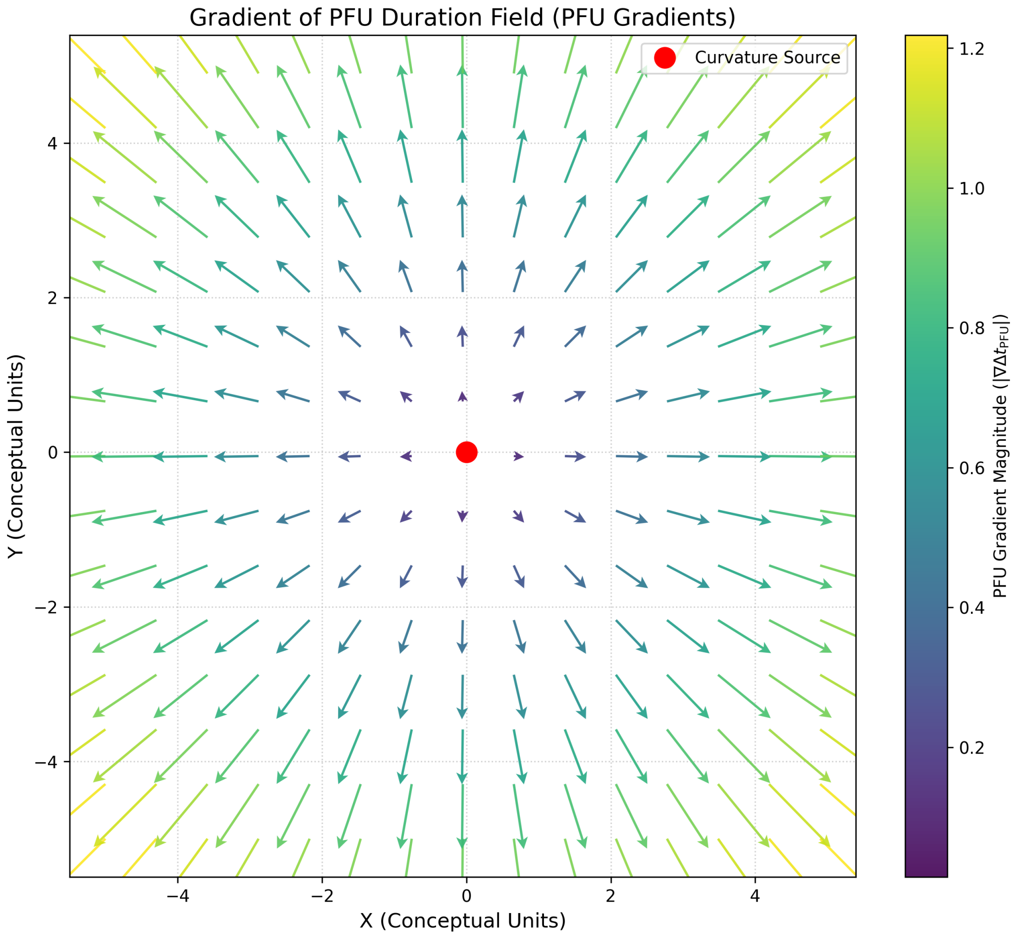

Figure 7: Depiction of the **PFU Gradient Vector Field** $\nabla\Delta t_{\text{PFU}}(x,t)$. Each arrow encodes a local PFU gradient: the orientation indicates the direction of the steepest increase in PFU duration (where time effectively *accelerates*), while the arrow color encodes the magnitude of this gradient. The central red region marks a localized source of intense projected curvature, where $\Delta t_{\text{PFU}} \to 0$ and time is effectively frozen. Outward-pointing arrows indicate that emergent time "speeds up" with increasing distance from this source.

As illustrated in Figure 7, PFU gradients form a coherent structure: arrows consistently emanate outward from the high-curvature source, representing steep increases in PFU duration. This captures the intuitive notion that emergent time flows more rapidly as one moves away from regions of maximal projection activity. The magnitude of the gradient, encoded in the color intensity, pinpoints locations where temporal progression is most non-uniform.

Thus, the Projected Curvature Field Tensor provides not only the mathematical underpinning of the framework but also a predictive handle on observable deviations in the *flow of time*, distinguishing the 4D Quantum Projection Framework from standard relativistic curvature and offering novel empirical avenues for testing.

C Glossary of Symbols

This appendix presents a categorized glossary of the principal symbols used throughout this work. Each entry provides a concise definition and contextual description relevant to the 4D Quantum Projection Hypothesis and the Entropion field framework.

C.1 Time, Projection, and PFU Parameters

Symbol	Description
Δt_{PFU}	Local PFU duration; fundamental discrete time interval for 3D projection of a 4D quantum state.
r	Projection rate; inverse of Δt_{PFU}.
r_0	Reference projection rate used as a normalization constant.
$\Gamma(x,t)$	Local decoherence rate induced by tracing out hidden dimensions.
Γ_H	Decoherence rate in highly coherent regions (slow entropy growth).
Γ_L	Decoherence rate in low-coherence regions (rapid entropy growth).
$d\tau$	Emergent proper time accumulated through sequential PFUs.
dt	External coordinate time parameter.
$\nabla\Delta t_{\mathrm{PFU}}$	Gradient of PFU duration, indicating the direction and magnitude of local projection-rate variation.
$\mathcal{P}(x,t)$	Projection curvature scalar; invariant derived from the Projected Curvature Field Tensor, quantifying curvature induced by 4D-to-3D projection.

C.2 Entropy and Thermodynamic Quantities

Symbol	Description
$S(x,t)$	von Neumann entropy of the reduced 3D density matrix $\rho_{3\mathrm{D}}$.
$\frac{dS}{dt}$	Rate of entropy production from non-unitary reduced dynamics.
$\phi(x,t)$	Entropion scalar field mediating entropy exchange and temporal asymmetry across the hidden dimension.

https://doi.org/10.33774/coe-2025-brblf-v2 **ORCID:** https://orcid.org/0009-0002-3862-6407

C.3 Geometry and Curvature Tensors

Symbol	Description
$\mathcal{R}^{P}_{\mu\nu\rho\sigma}$	Projected Curvature Field Tensor representing local geometric distortions generated by projection processes.
κ_c	Curvature–entropy coupling constant linking projection curvature to entropy gradients.

C.4 Quantum Dynamics and Operators

Symbol	Description
$\Psi(x^\mu, x^4, t)$	Full 4D wave function in extended Hilbert space including the hidden spatial coordinate.
$\rho_{3\mathrm{D}}$	Reduced 3D density matrix obtained by tracing out the hidden dimension.
H	Effective Hamiltonian governing reduced 3D dynamics.
$\hbar$	Reduced Planck constant.
$U(t)$	Unitary evolution operator describing closed-system quantum dynamics.

C.5 Quantum Clocks and Phase Variables

Symbol	Description
ω_{clock}	Proper frequency of an idealized quantum clock.
$\delta\omega(t)$	Projection-induced frequency shift arising from hidden-dimension coupling.
$\phi(t)$	Quantum phase of a clock oscillator or wave state.

C.6 Gravitational Spikes and Simulation Parameters

Symbol	Description
$h(t)$	Gravitational spike waveform used in conceptual simulations.

A_{spike}	Amplitude of the spike waveform.
ω_{spike}	Angular frequency of the oscillatory component of the spike.
ϕ_{spike}	Initial phase of spike oscillation.
τ_{decay}	Characteristic decay time of spike amplitude.
$V(t)$	External potential applied in simulation tests of projection-induced decoherence.

C.7 Fundamental Constants

Symbol	**Description**
c	Speed of light in vacuum.
k_B	Boltzmann constant.

References

[1] W. H. Zurek, "Decoherence, einselection, and the quantum origins of the classical," *Rev. Mod. Phys.*, vol. 75, no. 3, 2003, pp. 715–775. https://doi.org/10.1103/RevModPhys.75.715

[2] C. Rovelli, "Time in quantum gravity: An hypothesis," *Phys. Rev. D*, vol. 43, no. 2, 1991, pp. 442–456. https://doi.org/10.1103/PhysRevD.43.442

[3] A. Connes, "Noncommutative geometry and reality," *J. Math. Phys.*, vol. 36, no. 11, 1995, pp. 6194–6231. https://doi.org/10.1063/1.531241

[4] A. Ashtekar, T. Pawlowski, and P. Singh, "Quantum Nature of the Big Bang: Improved dynamics," *Phys. Rev. D*, vol. 74, no. 8, 2006, pp. 084003-1–084003-16. https://doi.org/10.1103/PhysRevD.74.084003

[5] The LIGO Scientific Collaboration and The Virgo Collaboration, "Observation of Gravitational Waves from a Binary Black Hole Merger," *Phys. Rev. Lett.*, vol. 116, no. 6, 2016, pp. 061102-1–061102-16. https://doi.org/10.1103/PhysRevLett.116.061102

[6] Z. Arzoumanian *et al.* (for the NANOGrav Collaboration), "The NANOGrav 12.5-year Data Set: Search For An Isotropic Stochastic Gravitational-Wave Background," *Astrophys. J. Lett.*, vol. 905, no. 2, 2020, pp. L34-1–L34-19. https://doi.org/10.3847/2041-8213/abd401

[7] A. Einstein, "Die Grundlage der allgemeinen Relativitätstheorie" (The Foundation of the General Theory of Relativity), *Annalen der Physik*, vol. 49, no. 7, 1916, pp. 769–822. https://doi.org/10.1002/andp.19163540702

[8] K. V. Kuchar, "Time and interpretations of quantum gravity," *Int. J. Mod. Phys. D*, vol. 20, no. 1, 2011, pp. 3–86. https://doi.org/10.1142/S0218271811019347

[9] C. J. Isham, "Canonical Quantum Gravity and the Problem of Time," 1992, Art. no. gr-qc/9210011. https://doi.org/10.48550/arXiv.gr-qc/9210011

[10] H. D. Zeh, *The Physical Basis of The Direction of Time*, 5th ed., The Frontiers Collection. Springer Berlin, Heidelberg, 2007. https://doi.org/10.1007/978-3-540-68001-7

[11] M. Schlosshauer, *Decoherence and the Quantum-To-Classical Transition*, 1st ed., The Frontiers Collection. Springer Berlin, Heidelberg, 2007. https://doi.org/10.1007/978-3-540-35775-9

[12] A. Sesana, "Prospects for Multiband Gravitational-Wave Astronomy after GW150914," *Phys. Rev. Lett.*, vol. 116, no. 23, 2016, pp. 231102-1–231102-6. https://doi.org/10.1103/PhysRevLett.116.231102

[13] A. S. Landsman *et al.*, "Ultrafast resolution of tunneling delay time," *Optica*, vol. 1, no. 5, 2014, pp. 343–349. https://doi.org/10.1364/OPTICA.1.000343

[14] W. M. Itano, D. J. Heinzen, J. J. Bollinger, and D. J. Wineland, "Quantum Zeno effect," *Phys. Rev. A*, vol. 41, no. 5, 1990, pp. 2295–2300. https://doi.org/10.1103/PhysRevA.41.2295

[15] J. Anders and M. Esposito, "Focus on quantum thermodynamics," *New J. Phys.*, vol. 19, no. 1, 2017, pp. 010201-1–010201-6. https://doi.org/10.1088/1367-2630/19/1/010201

[16] J. Magueijo, "Speedy sound and cosmic structure," *Phys. Rev. Lett.*, vol. 100, no. 23, 2008, pp. 231302-1–231302-4. https://doi.org/10.1103/PhysRevLett.100.231302

[17] B. Misra and E. C. G. Sudarshan, "The Zeno's paradox in quantum theory," *Journal of Mathematical Physics*, vol. 18, no. 4, 1977, pp. 756–763. https://doi.org/10.1063/1.523304

[18] A. Einstein, "On the Influence of Gravitation on the Propagation of Light," *Annalen der Physik*, vol. 35, no. 10, 1911, pp. 898–908. https://doi.org/10.1002/andp.19113401005

[19] B. F. Schutz, *A First Course in General Relativity*. Cambridge University Press, 2009. https://doi.org/10.1017/CBO9780511984181

[20] A. Messiah, *Quantum Mechanics*, vol. 2. North-Holland Publishing Company, 1961. https://books.google.ae/books?id=CXwfAQAAMAAJ

[21] R. M. Wald, *General Relativity*. The University of Chicago Press, 1984. https://doi.org/10.7208/chicago/9780226870373.001.0001

[22] C. W. Misner, K. S. Thorne, and J. A. Wheeler, *Gravitation*. W. H. Freeman, 1973. https://doi.org/10.1002/piuz.19750060209

[23] B. S. DeWitt, "Quantum Theory of Gravity. I. The Canonical Theory," *Phys. Rev.*, vol. 160, no. 5, 1967, pp. 1113–1148. https://doi.org/10.1103/PhysRev.160.1113

[24] A. Connes and C. Rovelli, "Von Neumann Algebra Automorphisms and Time-Thermodynamics Relation in General Covariant Quantum Theories," *Class. Quant. Grav.*, vol. 11, no. 12, 1994, pp. 2899–2918. https://doi.org/10.1088/0264-9381/11/12/007

[25] C. Rovelli, "Forget time," 2009, Art. no. arXiv:0903.3832. https://doi.org/10.48550/arXiv.0903.3832

[26] D. N. Page and W. K. Wootters, "Evolution without evolution: Dynamics described by stationary observables," *Phys. Rev. D*, vol. 27, no. 12, 1983, pp. 2885–2892. https://doi.org/10.1103/PhysRevD.27.2885

[27] J. Butterfield, "Julian Barbour The End of Time: The Next Revolution in Our Understanding of the Universe," *Br. J. Philos. Sci.*, vol. 53, no. 2, 2002, pp. 289–330. https://doi.org/10.1093/bjps/53.2.289

[28] C. Rovelli, *Quantum Gravity*. Cambridge University Press, 2010. https://doi.org/10.1017/CBO9780511755804

[29] J. Ambjorn, J. Jurkiewicz, and R. Loll, "Causal Dynamical Triangulations and the Quest for Quantum Gravity," in *Foundations of Space and Time*, G. Ellis, J. Murugan, and A. Weltman, Eds. Cambridge Univ. Press, 2010. https://doi.org/10.48550/arXiv.1004.0352

[30] R. Bousso, "The holographic principle," *Rev. Mod. Phys.*, vol. 74, no. 3, 2002, pp. 825–874. https://doi.org/10.1103/RevModPhys.74.825

[31] S. W. Hawking, "Particle creation by black holes," *Commun. Math. Phys.*, vol. 43, no. 3, 1975, pp. 199–220. https://doi.org/10.1007/BF02345020

[32] J. Preskill, "Do Black Holes Destroy Information?," in *Proc. Int. Symp. on Black Holes, Membranes, Wormholes, and Superstrings*, 1992, Art. no. hep-th/9209058. https://doi.org/10.48550/arXiv.hep-th/9209058

[33] R. Penrose and M. Gardner, *The Emperor's New Mind: Concerning Computers, Minds, and The Laws of Physics*. Oxford University Press, 1989. https://doi.org/10.1093/oso/9780198519737.001.0001

[34] T. D. Kieu, "The Second Law, Maxwell's Demon, and Work Derivable from Quantum Heat Engines," *Phys. Rev. Lett.*, vol. 93, no. 14, 2004, pp. 140403-1–140403-4. https://doi.org/10.1103/PhysRevLett.93.140403

[35] S. M. Carroll, *Spacetime and Geometry: An Introduction to General Relativity*. Cambridge University Press, 2019. https://doi.org/10.1017/9781108770385

[36] V. Vedral, *Decoding Reality: The Universe as Quantum Information*. Oxford University Press, 2018. https://doi.org/10.1093/oso/9780198815433.001.0001

[37] J. L. Lebowitz, "Boltzmann's Entropy and Time's Arrow," *Physics Today*, Sep. 1993. https://doi.org/10.1063/1.881363

[38] W. Greiner, L. Neise, and H. Stöcker, *Thermodynamics and Statistical Mechanics*. Springer, 1995. https://doi.org/10.1007/978-1-4612-0827-3

[39] J. S. Bell, "On the Einstein Podolsky Rosen Paradox," *Physics*, vol. 1, no. 3, 1964, pp. 195–200. https://doi.org/10.1103/PhysicsPhysiqueFizika.1.195

[40] A. Aspect, J. Dalibard, G. Roger, "Experimental Test of Bell's Inequalities Using Time-Varying Analyzers," *Physical Review Letters*, vol. 49, 1982, pp. 1804–1807. https://doi.org/10.1103/PhysRevLett.49.1804

[41] S. Weinberg, *Cosmology*. OUP Oxford, 2008. https://books.google.ae/books?id=2wlREAAAQBAJ

[42] A. H. Guth, "Inflationary Universe: A Possible Solution to the Horizon and Flatness Problems," *Physical Review D*, vol. 23, no. 2, 1981, pp. 347–356. https://doi.org/10.1103/PhysRevD.23.347

[43] A. D. Linde, "Chaotic Inflation," *Physics Letters B*, vol. 129, no. 3–4, 1983, pp. 177–181. https://doi.org/10.1016/0370-2693(83)90837-7

[44] W. H. Zurek, "Decoherence, Einselection, and the Quantum Origins of the Classical," *Reviews of Modern Physics*, vol. 75, 2003, pp. 715–775. https://doi.org/10.1103/RevModPhys.75.715

[45] G. 't Hooft, "Dimensional Reduction in Quantum Gravity," *arXiv preprint gr-qc/9310026*, 1993. https://arxiv.org/abs/gr-qc/9310026

[46] L. Susskind, "The World as a Hologram," *Journal of Mathematical Physics*, vol. 36, 1995, pp. 6377–6396. https://doi.org/10.1063/1.531249

[47] C. Barceló, S. Liberati, M. Visser, "Analogue Gravity," *Living Reviews in Relativity*, vol. 14, no. 3, 2011. https://doi.org/10.12942/lrr-2011-3

[48] Planck Collaboration, "Planck 2018 Results. VI. Cosmological Parameters," *Astronomy & Astrophysics*, vol. 641, A6, 2020. https://doi.org/10.1051/0004-6361/201833910

[49] National Institute of Standards and Technology (NIST), "CODATA Recommended Values of the Fundamental Physical Constants: 2022," 2022. https://physics.nist.gov/cuu/Constants/index.html

[50] D. J. Wineland, D. Leibfried, M. D. Barrett, A. Ben-Kish, J. C. Bergquist, R. B. Blakestad, J. J. Bollinger, J. Britton, J. Chiaverini, B. Demarco, D. Hume, W. M. Itano, M. Jensen, J. D. Jost, E. Knill, J. Koelemeij, C. Langer, W. Oskay, R. Ozeri, R. Reichle, T. Rosenband, T. Schaetz, P. O. Schmidt, and S. Seidelin, "Quantum control, quantum information processing, and quantum-limited metrology with trapped ions," in *Proc. Int. Conf. on Laser Spectroscopy (ICOLS)*, 2005, Art. no. quant-ph/0508025. https://doi.org/10.48550/arXiv.quant-ph/0508025

[51] A. J. Leggett, "Macroscopic Quantum Systems and the Quantum Theory of Measurement," *Progress of Theoretical Physics Supplement*, vol. 69, 1980, pp. 80–100. https://doi.org/10.1143/PTP.69.80

[52] A. D. Ludlow, M. M. Boyd, J. Ye, E. Peik, P. O. Schmidt, "Optical Atomic Clocks," *Reviews of Modern Physics*, vol. 87, 2015, pp. 637–701. https://doi.org/10.1103/RevModPhys.87.637

[53] J. M. Maldacena, "The Large-N Limit of Superconformal Field Theories and Supergravity," *International Journal of Theoretical Physics*, vol. 38, 1999, pp. 1113–1133. https://doi.org/10.1023/A:1026654312961

[54] J. Polchinski, *String Theory, Vol. 1: An Introduction to the Bosonic String.* Cambridge University Press, 2011. https://doi.org/10.1017/CBO9780511816079

[55] H.-P. Breuer and F. Petruccione, *The Theory of Open Quantum Systems.* Oxford University Press, 2007. https://doi.org/10.1093/acprof:oso/9780199213900.001.0001

[56] H. G. Winful, "Tunneling time, the Hartman effect, and superluminality: A proposed resolution of an old paradox," *Physics Reports*, vol. 436, no. 1, 2006, pp. 1–69. https://doi.org/10.1016/j.physrep.2006.09.002

[57] S. Haroche and J.-M. Raimond, *Exploring the Quantum: Atoms, Cavities, and Photons.* Oxford University Press, 2006. https://doi.org/10.1093/acprof:oso/9780198509141.001.0001

[58] M. H. Anderson, J. R. Ensher, M. R. Matthews, C. E. Wieman, and E. A. Cornell, "Observation of Bose-Einstein Condensation in a Dilute Atomic Vapor," *Science*, vol. 269, no. 5221, 1995, pp. 198–201. https://doi.org/10.1126/science.269.5221.198

[59] M. H. Devoret and R. J. Schoelkopf, "Superconducting Circuits for Quantum Information: An Outlook," *Science*, vol. 339, no. 6124, 2013, pp. 1169–1174. https://doi.org/10.1126/science.1231930

[60] J. J. Pla, K. Y. Tan, J. P. Dehollain, W. H. Lim, J. J. L. Morton, D. N. Jamieson, A. S. Dzurak, and A. Morello, "A single-atom electron spin qubit in silicon," *Nature*, vol. 489, no. 7417, 2012, pp. 541–545. https://doi.org/10.1038/nature11449

[61] J. Koch, T. M. Yu, J. Gambetta, A. A. Houck, D. I. Schuster, J. Majer, A. Blais, M. H. Devoret, S. M. Girvin, and R. J. Schoelkopf, "Charge-insensitive qubit design derived from the Cooper pair box," *Phys. Rev. A*, vol. 76, no. 4, 2007, pp. 042319-1–042319-19. https://doi.org/10.1103/PhysRevA.76.042319